The FASEB Journal
The Journal of the Federation of American Societies for Experimental Biology
All Articles | Submit | Subscribe | What's New | RSS

FASEB J. 2019 Jun; 33(6): 7348–7362. Published online 2019 Mar 8. doi: 10.1096/fj.201802510R: 10.1096/fj.201802510R

PMCID: PMC6529334 | PMID: 30848941

Disruption of both ROCK1 and ROCK2 genes in cardiomyocytes promotes autophagy and reduces cardiac fibrosis during aging

Jianjian Shi,[*,1] Michelle Surma,[*] Yang Yang,[*†] and Lei Wei[*‡,2]

[*]Herman B. Wells Center for Pediatric Research, Department of Pediatrics, School of Medicine, Indiana University, Indianapolis, Indiana, USA;
[†]Department of Cardiovascular Surgery, Xiangya Hospital, Central South University School of Medicine, Changsha, China; and
[‡]Department of Cellular and Integrative Physiology, School of Medicine, Indiana University, Indianapolis, Indiana, USA
[1]Correspondence: Herman B. Wells Center for Pediatric Research, Department of Pediatrics, School of Medicine, Indiana University, 1044 West Walnut St., R4-240, Indianapolis, IN 46202-5225, USA., E-mail: jishi@iu.edu
[2]Correspondence: Herman B. Wells Center for Pediatric Research, Department of Pediatrics, School of Medicine, Indiana University, 1044 West Walnut St., R4-370, Indianapolis, IN 46202-5225, USA., E-mail: lewei@iu.edu

Received 2018 Nov 21; Accepted 2019 Feb 18.

Abstract

In this study, we investigated the pathophysiological impact of Rho-associated coiled-coil–containing protein kinase (ROCK)1 and ROCK2 double deletion *vs.* single deletion on cardiac remodeling. Utilizing a cardiomyocyte-specific and tamoxifen-inducible MerCreMer recombinase (MCM), 3 mouse lines (MCM/ROCK1$^{fl/fl}$/ROCK2$^{fl/fl}$, MCM/ROCK1$^{fl/fl}$, and MCM/ROCK2$^{fl/fl}$) were generated. As early as 5 d after inducible deletion, the double ROCK knockout

reduced phosphorylation of myosin light chain (MLC) and focal adhesion kinase (FAK), supporting a role for ROCK activity in regulating the nonsarcomeric cytoskeleton. Moreover, the autophagy marker microtubule-associated proteins 1A-1B light chain 3B was increased in the double ROCK knockout, and these early molecular features persisted throughout aging. Mechanistically, the double ROCK knockout promoted age-associated or starvation-induced autophagy concomitant with reduced protein kinase B (AKT), mammalian target of rapamycin (mTOR), Unc-51–like kinase signaling, and cardiac fibrosis. In contrast, ROCK2 knockout hearts showed increased phosphorylated (p)-MLC and p-FAK levels, which were mostly attributable to a compensatory ROCK1 overactivation. Autophagy was inhibited at the baseline accompanying increased mTOR activity, leading to increased cardiac fibrosis in the ROCK2 knockout hearts. Finally, the loss of ROCK1 had no significant effect on p-MLC and p-FAK levels, mTOR signaling, or autophagy at baseline. In summary, deletions of ROCK isoforms in cardiomyocytes have different, even opposite, effects on endogenous ROCK activity and the MLC/FAK/AKT/mTOR signaling pathway, which is involved in autophagy and fibrosis of the heart.—Shi, J., Surma, M., Yang, Y., Wei, L. Disruption of both ROCK1 and ROCK2 genes in cardiomyocytes promotes autophagy and reduces cardiac fibrosis during aging.

Keywords: Rho kinase, cytoskeleton, mTOR

Rho-associated coiled-coil–containing protein kinases (ROCKs) are central regulators of the actin cytoskeleton downstream of the small GTPase RhoA (1–8). The 2 ROCK isoforms, ROCK1 and ROCK2, are highly homologous with an overall amino acid sequence identity of 65% (1–3). The best-characterized targets of ROCK in the vascular system and nonstriated muscle cells are myosin light chain (MLC) phosphatase, MLC (4–6), and LIM kinases (7, 8), thereby modulating actin cytoskeleton organization, stress fiber formation, and smooth-muscle cell contraction. Cardiomyocytes contain both sarcomeric and nonsarcomeric cytoskeleton, and the composition of the nonsarcomeric cytoskeleton appears to be similar to that of actin stress fibers and focal adhesions in nonstriated muscle cells (9–11). Although ROCK1 and ROCK2 are expressed in cardiomyocytes, their roles in regulating sarcomeric and nonsarcomeric cytoskeleton remain largely unexplained.

We previously found that ROCK1 is a key molecule in mediating apoptotic signaling in cardiomyocytes under pressure overload and in genetically induced pathologic

cardiac hypertrophy (12–16). Recently, we observed that ROCK1 deletion restores autophagic flux through reducing Beclin 1 phosphorylation in doxorubicin cardiotoxicity in global and cardiomyocyte-specific ROCK1 knockout mice (17). Collectively, these loss-of-function studies, along with other studies in genetically modified mouse models (18, 19), have provided strong evidence that ROCK1 is a vital player for pathologic cardiac fibrosis formation and cardiomyocyte apoptotic events but not for cardiac hypertrophy. On the other hand, global hemizygous ROCK2-deficient and cardiomyocyte-specific ROCK2-deficient mice were found to be resistant to angiotensin II and pressure overload–induced cardiac hypertrophy and fibrosis formation, supporting that ROCK2 is important in mediating the cardiac hypertrophic response (20, 21). Although these studies indicate a critical role of ROCKs in mediating cardiac function and remodeling, the fundamental question of whether ROCKs directly regulate sarcomeric and nonsarcomeric cytoskeleton in cardiomyocytes has not been addressed. Deletion of both ROCK isoforms in cardiomyocytes is therefore necessary to respond to this question.

The present study is focused on the roles of both ROCK1 and ROCK2 in cardiomyocytes using a cardiomyocyte-specific knockout approach achieved by tamoxifen (TAM)–inducible MerCreMer recombinase (MCM) (22). Three mouse models with double or single ROCK isoform knockout were generated for evaluating the impact of double *vs.* single isoform knockout under the same experimental conditions. Our results demonstrated that ROCKs are not required to maintain cardiac structure and function in adult hearts but are involved in regulating autophagy function through multiple mechanisms. This study also revealed a compensatory overactivation of ROCK1 in the ROCK2 knockout hearts, resulting in opposite effects on cardiac remodeling by ROCK2 deletion *vs.* double ROCK deletion in cardiomyocytes.

MATERIALS AND METHODS

Generation of mouse models

All animal experiments were conducted in accordance with the *Guide for the Care and Use of Laboratory Animals* (National Institutes of Health, Bethesda, MD, USA) and were approved by the Institutional Animal Care and Use Committee at the Indiana University School of Medicine. ROCK1$^{fl/fl}$ and ROCK2$^{fl/fl}$ mice were generated as previously described in refs. 17 and 23. Deletion of exon 5 in the ROCK1 gene by Cre

recombinase results in a frame-shift mutation, thus removing all residues from residue 137 to the end of the protein (**Fig. 1*A***). Deletion of exon 2 in the ROCK2 gene results in a frame-shift mutation, removing all residues from the residue 47 to the end of the protein (Fig. 1*A*). To generate cardiomyocyte-specific ROCK1 and ROCK2 knockout mice [α-myosin heavy chain (α-MHC)–Cre/ROCK1$^{fl/fl}$ and α-MHC–Cre/ROCK2$^{fl/fl}$], ROCK1$^{fl/fl}$ and ROCK2$^{fl/fl}$ mice were crossed to the α-MHC–Cre mice (24) and bred back to the ROCK1$^{fl/fl}$ and ROCK2$^{fl/fl}$ mice, respectively.

To generate inducible cardiomyocyte-specific ROCK1 knockout mice (MCM/ROCK1$^{fl/fl}$), ROCK1$^{fl/fl}$ mice were crossed to the transgenic mice expressing TAM-inducible Cre recombinase fused to mutant estrogen-receptor ligand-binding domain (MerCreMer) under the control of the α-MHC promoter MCM (22) and bred back to ROCK1$^{fl/fl}$ mice. To generate inducible cardiomyocyte-specific ROCK2 knockout mice (MCM/ROCK2$^{fl/fl}$), ROCK2$^{fl/fl}$ mice were crossed to the transgenic MCM mice (22) and bred back to ROCK2$^{fl/fl}$ mice. To generate double knockout mice, we first generated mice homozygous for the floxed ROCK1 and ROCK2 alleles (ROCK1$^{fl/fl}$/ROCK2$^{fl/fl}$ mice) by intercrossing ROCK1$^{fl/fl}$ and ROCK2$^{fl/fl}$ mice. ROCK1$^{fl/fl}$/ROCK2$^{fl/fl}$ mice were then crossed with the transgenic MCM mice and bred back to ROCK1$^{fl/fl}$/ROCK2$^{fl/fl}$ mice to produce inducible cardiac-specific double knockout mice (MCM/ROCK1$^{fl/fl}$/ROCK2$^{fl/fl}$). TAM (30 mg/kg dissolved in sunflower oil; MilliporeSigma, Burlington, MA, USA) was administrated to adult mice (3–6 mo old) of either sex by intraperitoneal injection once per day to induce knockout of ROCK1 and ROCK2. Hearts from MCM/ROCK1$^{fl/fl}$/ROCK2$^{fl/fl}$ mice subjected to 1–3 injections of TAM were collected 2–5 d after the first injection to determine the extent of ROCK1 and ROCK2 knockout (Figs. 1 and **2**). Control groups were MCM mice treated with TAM or oil and ROCK1$^{fl/fl}$/ROCK2$^{fl/fl}$ mice treated with TAM or oil. For starvation studies, mice were deprived of food for 24 h in clean cages, but they received water *ad libitum*.

Echocardiography analysis

Mouse cardiac dimensions and contractile functions were evaluated by noninvasive transthoracic echocardiography using a VisualSonics 2100 Ultrasound Machine for small-animal imaging and MS400 Transducer (Fujifilm, Tokyo, Japan). Functional parameters of the left ventricle were measured using standard assessment techniques as previously described in Shi *et al.* (13).

Histology and quantitative analysis

Total heart weight was indexed to tibial length. Cryosections or paraffin sections were stained with hematoxylin and eosin for initial evaluation and picrosirius red and fast green to identify collagen fibers as previously described in refs. 13, 14, 16, and 25. The quantification of collagen-stained area was performed with Image-Pro software (Media Cybernetics, Rockville, MD, USA). At least 10 randomly chosen high-power fields per section and 4 transverse sections from each heart, sampled from the midpoint between the apex and base, were analyzed.

Electron microscopy analysis

Ventricular specimens (cubes <3 mm square) fixed in 2.5% glutaraldehyde underwent sectioning and heavy metal uranyl acetate staining for contrast by the Electron Microscopy Center of the Indiana University School of Medicine. At least 6 separate sections from each group were analyzed. Electron micrographs were acquired on a Tecnai BioTwin transmission electron microscope (Thermo Fisher Scientific, Waltham, MA, USA) equipped with an Advanced Microscopy Techniques Charge-Coupled Device (AMT CCD) Camera (Advanced Microscopy Techniques, Woburn, MA, USA).

Protein analysis

Protein samples were prepared as previously described in refs. 13, 16, 17, and 25. Ventricular tissue fragments were disrupted with a Pyrex Potter-Elvehjem tissue grinder (Thermo Fisher Scientific) on ice in lysis buffer containing proteinase and phosphatase inhibitors (Roche, Basel, Switzerland). The homogenate was centrifuged at 15,000 *g* at 4°C for 15 min, and the supernatant was saved for immunoblotting. The blots were probed with primary antibodies to ROCK1 (sc-5560), ROCK2 (sc-5561), and focal adhesion kinase (FAK; sc-558) from Santa Cruz Biotechnology (Dallas, TX, USA); ROCK1 (4035), phosphorylated (p)-FAK-Tyr925 (3284), Bax (2772), microtubule-associated proteins 1A/1B light chain 3B (LC3) (2775), Beclin 1 (3738), p62 (5114), p-AMPK-Thr172 (2535), AMPK (2603), p-MLC-Ser19 (3671), MLC (672), p–protein kinase B (AKT)-Ser473 (9271), AKT (9272), p–mammalian target of rapamycin (mTOR)-Ser2448 (5536), and mTOR (2972) were from Cell Signaling Technology (Danvers, MA, USA); and p–Beclin 1-Thr119 (ABC118), p–Unc-51–like kinase (ULK)-Ser757 (ABC112), and ULK (ST1521) were from

MilliporeSigma. All blots were normalized to glyceraldehyde 3-phosphate dehydrogenase (GAPDH; ABS16; MilliporeSigma) or actin (MABT523; MilliporeSigma).

Gene expression analysis

Total RNA was extracted from ventricular tissues by using Trizol Reagent (Thermo Fisher Scientific). To assess mRNA transcript levels by real-time quantitative RT-PCR (qRT-PCR), cDNA was synthesized with a High-Capacity cDNA Reverse Transcription Kit (Thermo Fisher Scientific). TaqMan primers and probes for mouse GAPDH, ROCK1, ROCK2, α-MHC, βMHC, atrial natriuretic factor, B-type natriuretic peptide, and collagen 1α1 were from Thermo Fisher Scientific.

Statistical analysis

Data are reported as means ± SE. Comparisons between groups were analyzed by Student's *t* test or ANOVA as appropriate, with $P < 0.05$ considered as significant.

RESULTS

Generation of inducible cardiomyocyte-specific double ROCK knockout mice

To determine how the complete removal of ROCK activity in cardiomyocytes impacts cardiac structure and function, we first attempted to generate α-MHC–Cre/ROCK1$^{fl/fl}$/ROCK2$^{fl/fl}$ mice to make constitutive cardiomyocyte-specific knockout *via* α-MHC–Cre (24). Both α-MHC–Cre/ROCK1$^{fl/fl}$/ROCK2$^{+/fl}$ and α-MHC–Cre/ROCK1$^{+/fl}$/ROCK2$^{fl/fl}$ mice with only 1 wild-type (WT) allele of ROCK1 or ROCK2 gene remaining were viable up to 12 mo of age. We then crossed α-MHC–Cre/ROCK1$^{fl/fl}$/ROCK2$^{+/fl}$ or α-MHC–Cre/ROCK1$^{+/fl}$/ROCK2$^{fl/fl}$ mice with ROCK1$^{fl/fl}$/ROCK2$^{fl/fl}$ mice and we were unable to obtain any viable α-MHC–Cre/ROCK1$^{fl/fl}$/ROCK2$^{fl/fl}$ mice after screening over 200 mice after birth. These results indicated that complete removal of both ROCK1 and ROCK2 in cardiomyocytes leads to embryonic lethality. Therefore, the inducible approach *via* MCM (22) should be used to feasibly investigate the biological effects responding from double ROCK knockout in cardiomyocytes.

fl/fl fl/fl

We then generated MCM/ROCK1 /ROCK2 mice and established the optimal protocol for making inducible deletion of ROCK1 and ROCK2 in cardiomyocytes by TAM injection (Fig. 1). We observed that 2 or 3 doses of 30 mg/kg body weight TAM led to a reduction of >75% for ROCK1 and ROCK2 proteins (Fig. 1*B, C*) and a reduction of >80% for ROCK1 and ROCK2 mRNAs (Fig. 1*D*) in ventricular preparation 5 d after the first TAM dose compared with oil-injected mice, but not in other tissues including lung (Fig. 1*E*), confirming the tissue specificity of ROCK-gene disruption. In addition, the loss of protein levels of ROCK1 or ROCK2 was comparable to that observed in the α-MHC–Cre/ROCK1$^{fl/fl}$ or α-MHC–Cre/ROCK2$^{fl/fl}$ mouse hearts (Fig. 1*B*), supporting efficient cardiomyocyte-specific ROCK-gene disruption by this inducible protocol. Control mouse groups [MCM/ROCK1$^{fl/fl}$/ROCK2$^{fl/fl}$ mice treated with oil alone (Fig. 1*B–D*), MCM mice treated with TAM or oil (Fig. 1*E*), and ROCK1$^{fl/fl}$/ROCK2$^{fl/fl}$ mice treated with TAM or oil (Fig. 1*E*)] were used to confirm that there were no nonspecific toxic effects of TAM or Cre activity. The TAM doses used in this study were lower than reported doses, which could induce cardiac toxicity in the presence of MCM (26–28). Because 3 doses of TAM gave no detectable toxic effects on cardiac function monitored by echocardiography at d 5, 10, and 30 after the first injection of TAM, we subsequently used this dosage to ensure maximal reduction of both ROCK1 and ROCK2 proteins in MCM/ROCK1$^{fl/fl}$/ROCK2$^{fl/fl}$ mice treated with TAM; we used MCM/ROCK1$^{fl/fl}$/ROCK2$^{fl/fl}$ mice treated with oil or MCM mice treated with TAM as control groups in the subsequent experiments.

Early molecular changes associated with inducible cardiomyocyte-specific double ROCK knockout

We next assessed the impact of double ROCK deletion on the phosphorylation of molecules in several known ROCK downstream substrates. Interestingly, we observed a temporary reduction of MLC and FAK phosphorylation levels associated with reduced ROCK1 and ROCK2 expression levels in cardiomyocytes, and this effect was noticeable at d 2 after the first dose of TAM and reached maximal levels at d 5 (Fig. 2*A–C*). These observations indicate that ROCK activity in cardiomyocytes regulates the nonsarcomeric cytoskeleton, which appears to be similar to that of actin stress fibers and focal adhesions in nonstriated muscle cells (9). Moreover, an increase in autophagy marker LC3-II accumulation was also observed (Fig. 2*A, C*), suggesting that ROCK activity in cardiomyocytes is involved in regulating autophagy function.

Late molecular changes associated with inducible cardiomyocyte-specific double ROCK knockout

To further investigate the impact of deletion of both ROCK1 and ROCK2 on cardiac structure and function, we evaluated molecular changes in a time course of 1, 6, or 12 mo beginning from the first TAM injection, which was performed in MCM/ROCK1$^{fl/fl}$/ROCK2$^{fl/fl}$ mice at 6 mo old, followed by collecting the hearts at 7, 12, or 18 mo old. The previously observed molecular changes at early time points including p-MLC, p-FAK, and LC3-II were reversed at the 1-mo time point post-TAM injection, except for the reduced ROCK1 and ROCK2 expression (Fig. 2*D*), suggesting the presence of compensatory effects that are due to other unknown signaling pathways. However, these compensatory effects were temporary because the reduced p-MLC and p-FAK levels and increased LC3-II levels recurred at later 6- and 12-mo time points (Fig. 2*D–F*). Among the numerous examined autophagy-related molecules, we noticed that increased LC3-II levels were associated with reduced phosphorylation of mTOR in the double ROCK knockout hearts (Fig. 2*F*). Because the activation of the mTOR signaling pathway inhibits autophagy function (29–31), the reduced mTOR activity as indicated by reduced p-mTOR levels likely contributes to the increased LC3-II levels found in the double ROCK knockout hearts.

Inducible cardiomyocyte-specific double ROCK knockout inhibits age-related cardiac fibrosis

From histologic analyses, reduced collagen deposition was observed during the aging process in the double ROCK knockout hearts at 12 mo post-TAM injection (at 18 mo of age) (**Fig. 3*A, B***), consistent with reduced collagen 1 α1 gene expression (Fig. 3*C*) and decreased smooth-muscle α-actin levels (Fig. 2*D, F*). Because increased autophagy was observed at the 6–12-mo time points post-TAM injection in the double ROCK knockout mice, it most likely contributes to the reduced cardiac fibrosis during aging. It should be noted that the increases in heart weight (Fig. 3*D*) and cardiac fibrosis during this aging period did not display significant effects on cardiac contractile function (Fig. 3*E, F*), as indicated by an insignificant decrease in left ventricular fractional shortening (Fig. 3*F*) and insignificant changes in lung weight (Fig. 3*E*), which is an indicator for lung congestion, between the 2 time points of 1 and 12 mo in the control group and in the double ROCK knockout group. The findings indicated that the cardiac remodeling remained in a compensatory stage.

Inducible cardiomyocyte-specific double ROCK knockout promotes starvation-induced autophagy through inhibiting mTOR signaling

To further investigate the mechanisms underlying the increased autophagy function in the double ROCK knockout hearts, we examined autophagy activity in mouse hearts after exposing mice to starvation. As already mentioned (Fig. 2*D*), the molecular changes were minimal between the double ROCK knockout and control mice at 1 mo post-TAM injection, except for the differences in ROCK1 and ROCK2 expression. We therefore applied starvation stress at this time point to minimize the preexisting effects of the double ROCK deletion on autophagy and related pathways (Fig. 4*A*). We observed increased LC3-II levels in the control mouse hearts after 24 h of starvation (**Fig. 4*B, C***), which was associated with increased phosphorylation of AMPK (Fig. 4*B, D*). However, the activity of the mTOR signaling pathway, as reflected by p-mTOR levels and the phosphorylation of ULK on Ser757 (a downstream effector of mTOR in inhibiting autophagy), was not significantly affected by starvation in the control group (Fig. 4*B, D*). In contrast, a further increased starvation-induced autophagy function was detected in double ROCK knockout mouse hearts (Fig. 4*A*), associated with reduced p-mTOR and p-ULK-Ser757 levels (Fig. 4*B, D*), supporting the notion that reduced mTOR signaling is involved in activating autophagy function of the double ROCK knockout hearts. We next examined the upstream of mTOR signaling; the decreased phosphorylation of AKT on Ser473 in the double ROCK knockout hearts, parallel to the reduced p-MLC and p-FAK levels, suggests that the increased autophagy in cardiomyocytes of double ROCK deletion is through inhibiting the MLC/FAK/AKT/mTOR/ULK pathway rather than increasing AMPK activity, which was found to be similar in both starved control and double knockout hearts. It is worth noting that the inhibition of this pathway was not detected in either ROCK1 or ROCK2 single knockout hearts (see below); in other words, these were unique characteristics found in double ROCK deletion.

Early molecular changes associated with inducible cardiomyocyte-specific single ROCK knockout

To compare the impact of double ROCK knockout *vs.* ROCK1 or ROCK2 single knockout in cardiomyocytes, parallel experiments were performed in MCM/ROCK1$^{fl/fl}$ and MCM/ROCK2$^{fl/fl}$ mice. These mice received 3 doses of TAM at 30 mg/kg body weight, and the molecular changes were evaluated at d 5 after the first

dose (**Fig. 5*A, B***). Different from the double ROCK knockout mice, the p-MLC, p-FAK, and LC3-II levels were unchanged in the ROCK1 knockout hearts (Fig. 5*A, C*), suggesting that the presence of ROCK2 in the ROCK1 knockout cardiomyocytes is able to maintain the nonsarcomeric cytoskeleton. Also different from the double ROCK knockout mice, the p-MLC and p-FAK levels were increased in the ROCK2 knockout hearts, and this increase in p-MLC and p-FAK levels was associated with a decrease in LC3-II levels (Fig. 5*A, C*).

Consistent with the inducible ROCK2 knockout mice, the p-MLC and p-FAK levels were also increased in the constitutive α-MHC–Cre/ROCK2$^{fl/fl}$ ROCK2 knockout hearts at 3 wk of age, and this increase in p-MLC and p-FAK levels was associated with decreased LC3-II levels (Fig. 5*D*). Selection of the young α-MHC–Cre/ROCK2$^{fl/fl}$ mice for this experiment is because of the reported cardiac toxicity appearing in α-MHC–Cre mice by 3 mo of age compared with WT littermates (32). We have noted that α-MHC–Cre alone had no significant effects on p-MLC, p-FAK, and LC3-II at 3 wk of age (unpublished results). Together, these results suggest a compensatory increase in ROCK1 activity in the absence of ROCK2 and further support a role for ROCK activity in regulating autophagy in cardiomyocytes.

Inducible cardiomyocyte-specific ROCK1 knockout reduces starvation-induced autophagy through inhibiting Beclin 1 phosphorylation

We have previously reported that systemic ROCK1 deletion and constitutive cardiomyocyte-specific ROCK1 deletion *via* α-MHC–Cre reduced phosphorylation levels of Beclin 1 at Thr119 and improved autophagic flux in doxorubicin-treated hearts through inhibiting Beclin 1–mediated autophagy initiation (17). In addition, autophagy was not affected at the baseline in these constitutive ROCK1 knockout models (17), similar to the present inducible ROCK1 knockout model (Fig. 5*A*). To determine the role of ROCK1 in Beclin 1–mediated autophagy in the inducible knockout model, we examined autophagy activity in MCM/ROCK1$^{fl/fl}$ hearts after stressing with starvation (**Fig. 6**). Like the experiments performed with the double ROCK knockout mice, the starvation stress was applied at 1 mo post-TAM injection to MCM/ROCK1$^{fl/fl}$ mice. Interestingly, p–Beclin 1 levels were significantly reduced in the starved ROCK1 knockout hearts but not in control hearts, which is associated with reduced LC3-II levels (Fig. 6*A, B*) compared with the starved control hearts. Moreover, different from the double ROCK knockout hearts, the levels of p-MLC, p-FAK, p-AKT, p-mTOR, and p-ULK were not reduced in the starved ROCK1 knockout

hearts (Fig. 6*A*), indicating that the presence of ROCK2 in the ROCK1 knockout cardiomyocytes is able to maintain mTOR activity at the baseline and under starvation. It is worth noting that although both ROCK1 deletion (Fig. 6*A, B*) and double ROCK deletion (Fig. 4*B*) showed reduced Beclin 1 phosphorylation, they had opposite effects on autophagy, suggesting that the suppressed mTOR activity in the double ROCK knockout hearts has a dominant effect on autophagy function.

Inducible cardiomyocyte-specific ROCK2 knockout increases ROCK1 activity, inhibits autophagy, and induces cardiac fibrosis

Because inducible ROCK2 deletion in cardiomyocytes resulted in an increase in p-MLC and p-FAK levels associated with a decrease in LC3-II levels at d 5 from the first dose of TAM (Fig. 5), we performed a time-course study following these molecular changes at 1, 3, or 6 mo after TAM injection (**Fig. 7**). These MCM/ROCK2$^{fl/fl}$ mice received either TAM or oil injection at 6 mo, and the hearts were collected at 7, 9, or 12 mo. The increased p-MLC and p-FAK levels and reduced LC3-II levels that were observed at d 5 persisted at these later time points (Fig. 7*A, B*) and were associated with increased p-mTOR levels (Fig. 7*A, B*), supporting increased ROCK1 activity and reduced autophagy function, which resulted from activating the mTOR pathway in the ROCK2 knockout cardiomyocytes. Importantly, smooth-muscle α-actin levels increased at 6 mo from the first dose of TAM (Fig. 7*A, B*), suggesting that the persistent ROCK1 overactivation promotes cardiac fibrosis at baseline conditions. This profibrosis feature at 6 mo post-TAM was only observed in the ROCK2 knockout hearts and not in the ROCK1 knockout hearts (Fig. 7*A*).

Consistent with the increased smooth-muscle α-actin levels at 6 mo post-TAM injection, increased collagen deposition (**Fig. 8*A, B***) was also observed in the ROCK2 knockout hearts associated with increased heart weight (Fig. 8*C*), supporting the notion that impaired autophagy caused by persistent ROCK1 and mTOR activation contributes to cardiac fibrosis and hypertrophy in the ROCK2 knockout hearts. Despite the increases in heart weight and cardiac fibrosis at 6 mo after ROCK2 knockout, the cardiac contractile function was preserved because no significant increase in lung weight (Fig. 8*D*) and no significant decrease in left ventricular fractional shortening (Fig. 8*E*) were detected between ROCK2 knockout and control mice, indicating that the cardiac remodeling remained at a compensatory stage. Together, these results not only reveal a compensatory increase of ROCK1 activity because of ROCK2 ablation, but they also support a direct role for cardiomyocyte

ROCK overactivation in inhibiting autophagy activity, which can have a long-term consequence on cardiac fibrotic remodeling.

DISCUSSION

The present study examined the short- and long-term impacts of double ROCK deletion *vs.* single ROCK isoform knockout *via* an inducible approach in cardiomyocytes on cardiac structure and function. This study demonstrated that double or single ROCK isoforms deletion in cardiomyocytes resulted in different outcomes on endogenous ROCK activity, autophagic activity, and cardiac fibrosis (**Fig. 9**). We observed that the endogenous ROCK activity in cardiomyocytes can be monitored by measuring the phosphorylation of MLC, which is critically involved in FAK activation. Because MLC is present in the nonsarcomeric cytoskeleton of cardiomyocytes and in the cytoskeleton of all other cell types in the heart, our results provide direct evidence that ROCK activity regulates nonsarcomeric cytoskeleton organization in cardiomyocytes, which has numerous important functions, including proper assembly and maintenance of myofibrils, maintenance of sarcolemma integrity, and interaction with other cardiomyocytes, the extracellular matrix, other noncardiomyocytes, *etc.* (9–11). The primary effects of inducible ablation of ROCK proteins could be observed 2–5 d post-TAM injection (prior to cardiac remodeling); phosphorylation of MLC and FAK was only reduced in the double ROCK knockout hearts but remained unchanged in the ROCK1 knockout hearts and increased in the ROCK2 knockout hearts, which is likely attributable to a compensatory overactivation of ROCK1. Interestingly, the reduced phosphorylation of MLC and FAK was reversed at 1 mo post-TAM injection in the double ROCK knockout hearts, indicating that compensation can occur through the action of other kinases. This observation can be explained by the fact that the consensus sequences Arg/Lys-X-Ser/Thr or Arg/Lys-X-X-Ser/Thr (R/KXS/T or R/KXXS/T, respectively) of ROCK phosphorylation sites can also be phosphorylated by several other protein kinase A, G, C (AGC) family of serine and threonine protein kinases (33, 34). However, the reduced phosphorylation of MLC and FAK reappeared during aging or exposure to starvation stress, indicating that this compensation is only temporary and has a limited effect. Hence, we demonstrated that the inducible double ROCK knockout mice can serve as a valid tool to determine the endogenous ROCK substrates in cardiomyocytes, presenting advantages compared to ROCK chemical inhibitors which inhibit ROCK activity in all cell types of the heart, and even nonspecifically inhibit other kinases.

Our study demonstrates that ROCKs in cardiomyocytes of adult mouse hearts are not required for maintaining cardiac structure and function but are required during mouse heart development, as evidenced by the inability to obtain viable α-MHC–Cre/ROCK1$^{fl/fl}$/ROCK2$^{fl/fl}$ mice after birth. However, we noticed that both α-MHC/ROCK1$^{fl/fl}$/ROCK2$^{+/fl}$ and α-MHC/ROCK1$^{+/fl}$/ROCK2$^{fl/fl}$ mice were viable with normal cardiac structure and function at weaning ages; this finding indicates that only 1 allele of the ROCK1 or ROCK2 gene in cardiomyocytes is sufficient for processing heart development. In addition to the embryonic lethality associated with the constitutive α-MHC–Cre–mediated deletion of both ROCKs, α-MHC–Cre transgenic mice have been reported to exhibit signs of cardiac toxicity by 3 mo of age and exhibit decreased cardiac function by 6 mo of age compared with WT littermates (32). The inducible approach used in the current study allowed bypassing not only the critical developmental window requiring the presence of at least 1 ROCK allele but also the cardiotoxicity of α-MHC–Cre for the longitudinal study.

Our study provided strong evidence that cardiomyocyte ROCKs play a critical role in modulating autophagy function, which chronically affects cardiac fibrotic remodeling. Double ROCK knockout hearts exhibited increased autophagy immediately after ablation of ROCK proteins, which also existed persistently during aging, resulting in reduced cardiac fibrotic remodeling (Fig. 9*A*). Mechanistically, suppressed MLC/FAK/AKT/mTOR signaling was observed in the double ROCK knockout heart during aging (Fig. 2) and in starvation-induced autophagy activation (Fig. 4), revealing a novel functional connection between ROCK-mediated MLC phosphorylation and mTOR signaling; the former modulates nonsarcomeric cytoskeleton, and the latter inhibits autophagy activity. In line with our results, previous studies suggest that RhoA and ROCK mediate the activation of FAK, which associates with the regulatory p85 subunit of PI3K, activating it to mediate downstream activation of AKT in cultured neonatal cardiomyocytes (35, 36). In addition, our results are consistent with the previously reported inverse relationship between autophagy and cardiac fibrosis during aging, attributable to elevated mTOR activity; such a decline of autophagy induces accumulation of misfolded proteins, dysfunctional organelles, and increased oxidative stress, which facilitate senescence in the heart and increase cardiac fibrosis and other abnormalities (30, 31, 37–39). Because increased oxidative stress and accumulation of damaged proteins and organelles in the heart also occur in response to pathologic insults, including pressure overload, ischemic injury, and both genetic and metabolic cardiomyopathies

in which partial genetic or pharmacological inhibition of mTOR signaling is beneficial (31), double ROCK deletion in the heart is anticipated to exert beneficial effects during cardiac stress through inhibiting mTOR activity and facilitating autophagy. Because the remaining ROCK isoform in the single ROCK knockout cardiomyocytes is able to increase mTOR activity (ROCK2 knockout model, Fig. 9*B*) or maintain mTOR activity (ROCK1 knockout model, Fig. 9*C*), the double ROCK deletion model is expected to produce more prominent cardioprotective effects than the single ROCK deletion models in response to cardiac stress, in which decreased mTOR signaling is beneficial. Future studies are warranted to study the effects of double ROCK deletion in various stress contexts.

Studies using genetically modified mouse models have demonstrated the contribution of cardiomyocyte RhoA and ROCK activation to the development of fibrosis in response to pathologic stress (12, 14, 16, 18, 19, 40, 41). Deletion of RhoA (40) or Rho guanine nucleotide exchange factor 12 in cardiomyocytes (41) has anti-fibrotic effects in response to pressure overload because of inhibition of RhoA and, presumably, ROCKs. Global homozygous ROCK1$^{-/-}$ (12) and heterozygous ROCK1$^{+/-}$ (19) mice show decreased cardiac fibrosis without affecting pressure overload or angiotensin II–induced cardiac hypertrophy. In a gain-of-function mouse model, transgenic mice expressing constitutively active ROCK in cardiomyocytes develop fibrotic cardiomyopathy under physiologic conditions, which is further augmented by angiotensin II stimulation (18). Several potential mechanisms have been proposed to link RhoA and ROCK activation in cardiomyocytes with increased cardiac fibrosis under pathologic stress, which are as follows: *1*) replacement cardiac fibrosis that is due to ROCK1-mediated cardiomyocyte apoptosis (14, 16); *2*) increased transcriptional activation of genes involved in fibrosis that is due to increased RhoA- and ROCK-mediated F-actin assembly, including myocardin response transcription factor and serum response factor, resulting in increased production of fibrogenic cytokines such as TGF-β1 and connective tissue growth factor in cardiomyocytes, which leads to increased fibrotic response in cardiac fibroblasts (12, 18, 19, 40); and *3*) increased NF-κB–mediated inflammatory response in cardiomyocytes (18). The following difference between the current study and the previous studies should be noted: there were no clear differences reported in cardiac structure and function from previous loss-of-function mouse models compared with control mice under physiologic conditions (12, 14, 16, 18, 19, 40, 41). The potential explanation could be the differences in ages of mice and time frames of the experiments; a 12-mo-long time frame was followed in the present study to detect phenotype differences under

physiologic conditions in the double ROCK deletion model at 18 mo of age. In addition, the protective mechanisms, such as increased autophagy associated with reduced mTOR signaling, have not been reported in previous studies. Future studies are warranted to study the effects of double ROCK deletion in cardiomyocytes on serum response factor–mediated fibrotic response under pathologic conditions and the effects of double ROCK deletion in other cell types, including cardiac fibroblasts and vascular cells.

Recently, we observed that global ROCK1 deletion or cardiomyocyte-specific deletion by crossing with α-MHC–Cre transgenic mice restores autophagic flux through reducing Beclin 1 phosphorylation in doxorubicin cardiotoxicity (17). In the present study, inducible loss of ROCK1 had an insignificant effect on MLC/FAK/AKT/mTOR signaling and autophagy at the baseline (Fig. 9*C*) but reduced starvation-induced autophagy associated with reduced Beclin 1 phosphorylation (Fig. 6), which is consistent with the reported starvation-mediated autophagic response in global ROCK1 knockout mouse hearts (42). On the other hand, despite the reduced Beclin 1 phosphorylation in the double knockout hearts, autophagy was still increased because of reduced MCL/FAK/AKT/mTOR signaling (Figs. 4*B* and 9*A*). Together, these findings reveal that ROCK activity can modulate autophagy in cardiomyocytes *via* several mechanisms, and MLC/FAK/AKT/mTOR signaling appears to have a dominant effect over the Beclin 1 signaling.

In addition to the ROCK1-mediated phosphorylation of Beclin 1 (17, 42), other studies have demonstrated both positive (43, 44) and negative (45) effects of ROCK inhibition on autophagy. Treatment with the ROCK inhibitor Y27632 increased the degradation of mutant Huntington protein *via* proteasome degradation and autophagy in mouse neuroblastoma cell lines (44). ROCK inhibition has also been linked to an increase in autophagy responding to starvation or rapamycin treatment and is associated with the formation of enlarged early autophagosomes and late degradative autolysosomes in human embryonic kidney 293 cells (43). In contrast, ROCK inhibition impaired the starvation-mediated autophagic response in HeLa cells and CHO cells through its inhibitory effect on actin cytoskeleton formation, which participates in the initial membrane remodeling at very early stages of autophagosome formation (45). These context-dependent roles of ROCK in modulating autophagy are likely because of the complexity of autophagy regulation and the variety of cellular functions controlled by RhoA and ROCK signaling. Our study uncovered both positive (through mTOR signaling) and negative (through

Beclin 1 signaling) effects of ROCK inhibition in cardiomyocytes on autophagy function, therefore providing mechanistic explanation for the potential opposite effects on autophagy.

In contrast with the double ROCK knockout, inducible ROCK2 knockout caused compensatory ROCK1 overactivation in both the short and long term, resulting in increased MLC/FAK/AKT/mTOR signaling, decreased autophagy, and increased age-related cardiac fibrosis and hypertrophy (Fig. 9*B*). This observation provides further support for a ROCK-mediated regulation of mTOR signaling, which impacts autophagy and fibrosis. In addition, increased fibrosis accompanying increased ROCK activity is consistent with the profibrotic effects of increased ROCK activity observed in a cardiomyocyte-specific overexpression of the ROCK1 mouse model (18). However, the detrimental effects of ROCK2 deletion observed in our study are different from the antifibrotic and antihypertrophic phenotypes reported in the cardiomyocyte-specific ROCK2 knockout by crossing with α-MHC–Cre transgenic mice under pressure overload (20, 21). This discrepancy can be explained by the different knockout approaches, stresses, and time frames between these studies (*e.g.*, aging-related stress and 6-mo follow-up in our study *vs.* pressure-overload stress and 4-wk follow-up in others) (20, 21). As previously mentioned, α-MHC–Cre transgenic mice have been reported to exhibit signs of cardiac toxicity by 3 mo of age and decreased cardiac function associated with increased fibrosis and inflammation by 6 mo compared with WT littermates, which is because of DNA damages caused by constitutive Cre activity (32); therefore, these mice are not appropriate for a longitudinal study. It is important to note that we have indeed observed increased MLC phosphorylation in α-MHC–Cre/ROCK2$^{fl/fl}$ hearts as early as 3 wk of age (Fig. 5*D*), and this time point is before the onset of signs of cardiac toxicity from 3 to 6 mo of age. Therefore, a compensatory overactivation of ROCK1 in the absence of ROCK2 cannot be overlooked. Further investigation will determine whether inducible ROCK2 deletion provides beneficial or detrimental responses to pressure overload and other pathologic stresses.

In summary, we have discovered *in vivo* short- and long-term impacts of double or single ROCK deletion in cardiomyocytes and demonstrated that ROCKs are not required for maintaining cardiac structure and function in adult hearts, but they participate in the regulation of nonsarcomeric cytoskeleton organization and autophagy function through multiple mechanisms, such as an mTOR-mediated inhibiting pathway and a Beclin 1–mediated activating pathway. The present study

also revealed a compensatory overactivation of ROCK1 in the ROCK2 knockout hearts. Consequently, cardiac remodeling processes can present varied, even opposite, outcomes, depending on double ROCK deletion *vs.* single ROCK1 or ROCK2 deletion in cardiomyocytes.

ACKNOWLEDGMENTS

The authors thank the Transgenic and Knock-Out Mouse Core, the Small Animal Ultrasound Core, and the Electron Microscopy Center at the Indiana University School of Medicine for assistance in the generation of Rho-associated coiled-coil–containing protein kinase (ROCK1)$^{fl/fl}$ and ROCK2$^{fl/fl}$ mice, echocardiography imaging, and electron microscopy imaging. This work was supported by U.S. National Institutes of Health, National Heart, Lung, and Blood Institute Grants HL107537 and HL134599; a Grant-in-Aid award from the American Heart Association, Midwest Affiliate (12GRNT12060525); and the Riley Children's Foundation (to L.W.). It was also supported by a Biomedical Research Grant from the Indiana University School of Medicine (2286128ZJ to J.S.) The authors declare no conflicts of interest.

Glossary

α-MHC	α-myosin heavy chain
AKT	protein kinase B
FAK	focal adhesion kinase
GAPDH	glyceraldehyde 3-phosphate dehydrogenase
LC3	microtubule-associated proteins 1A/1B light chain 3B
MCM	MerCreMer recombinase
MLC	myosin light chain

mTOR	mammalian target of rapamycin
qRT-PCR	quantitative RT-PCR
ROCK	Rho-associated coiled-coil–containing protein kinase
TAM	tamoxifen
ULK	Unc-51–like kinase
WT	wild type

AUTHOR CONTRIBUTIONS

J. Shi and L. Wei designed research; J. Shi, M. Surma, Y. Yang, and L. Wei performed research; J. Shi, M. Surma, Y. Yang, and L. Wei analyzed data; and J. Shi and L. Wei wrote the paper.

REFERENCES

1. Matsui T., Amano M., Yamamoto T., Chihara K., Nakafuku M., Ito M., Nakano T., Okawa K., Iwamatsu A., Kaibuchi K. (1996) Rho-associated kinase, a novel serine/threonine kinase, as a putative target for small GTP binding protein Rho. *EMBO J.* 15, 2208–2216 10.1002/j.1460-2075.1996.tb00574.x [PMCID: PMC450144] [PubMed: 8641286] [CrossRef: 10.1002/j.1460-2075.1996.tb00574.x]

2. Ishizaki T., Maekawa M., Fujisawa K., Okawa K., Iwamatsu A., Fujita A., Watanabe N., Saito Y., Kakizuka A., Morii N., Narumiya S. (1996) The small GTP-binding protein Rho binds to and activates a 160 kDa Ser/Thr protein kinase homologous to myotonic dystrophy kinase. *EMBO J.* 15, 1885–1893 10.1002/j.1460-2075.1996.tb00539.x [PMCID: PMC450107] [PubMed: 8617235] [CrossRef: 10.1002/j.1460-2075.1996.tb00539.x]

3. Nakagawa O., Fujisawa K., Ishizaki T., Saito Y., Nakao K., Narumiya S. (1996) ROCK-I and ROCK-II, two isoforms of Rho-associated coiled-coil forming protein serine/threonine kinase in mice. *FEBS Lett.* 392, 189–193 10.1016/0014-5793(96)00811-3 [PubMed: 8772201] [CrossRef: 10.1016/0014-5793(96)00811-3]

4. Amano M., Chihara K., Kimura K., Fukata Y., Nakamura N., Matsuura Y., Kaibuchi K. (1997) Formation of actin stress fibers and focal adhesions enhanced by Rho-kinase. *Science* 275, 1308–1311 10.1126/science.275.5304.1308 [PubMed: 9036856] [CrossRef: 10.1126/science.275.5304.1308]

5. Kimura K., Ito M., Amano M., Chihara K., Fukata Y., Nakafuku M., Yamamori B., Feng J., Nakano T., Okawa K., Iwamatsu A., Kaibuchi K. (1996) Regulation of myosin phosphatase by Rho and Rho-associated kinase (Rho-kinase). *Science* 273, 245–248 10.1126/science.273.5272.245 [PubMed: 8662509] [CrossRef: 10.1126/science.273.5272.245]

6. Leung T., Chen X. Q., Manser E., Lim L. (1996) The p160 RhoA-binding kinase ROK alpha is a member of a kinase family and is involved in the reorganization of the cytoskeleton. *Mol. Cell. Biol.* 16, 5313–5327 10.1128/MCB.16.10.5313 [PMCID: PMC231530] [PubMed: 8816443] [CrossRef: 10.1128/MCB.16.10.5313]

7. Maekawa M., Ishizaki T., Boku S., Watanabe N., Fujita A., Iwamatsu A., Obinata T., Ohashi K., Mizuno K., Narumiya S. (1999) Signaling from Rho to the actin cytoskeleton through protein kinases ROCK and LIM-kinase. *Science* 285, 895–898 10.1126/science.285.5429.895 [PubMed: 10436159] [CrossRef: 10.1126/science.285.5429.895]

8. Arber S., Barbayannis F. A., Hanser H., Schneider C., Stanyon C. A., Bernard O., Caroni P. (1998) Regulation of actin dynamics through phosphorylation of cofilin by LIM-kinase. *Nature* 393, 805–809 10.1038/31729 [PubMed: 9655397] [CrossRef: 10.1038/31729]

9. Kee A. J., Gunning P. W., Hardeman E. C. (2009) Diverse roles of the actin cytoskeleton in striated muscle. *J. Muscle Res. Cell Motil.* 30, 187–197 10.1007/s10974-009-9193-x [PubMed: 19997772] [CrossRef: 10.1007/s10974-009-9193-x]

10. Henderson C. A., Gomez C. G., Novak S. M., Mi-Mi L., Gregorio C. C. (2017) Overview of the muscle cytoskeleton. *Compr. Physiol.* 7, 891–944 10.1002/cphy.c160033 [PMCID: PMC5890934] [PubMed: 28640448] [CrossRef: 10.1002/cphy.c160033]

11. Ehler E. (2018) Actin-associated proteins and cardiomyopathy-the ‘unknown’ beyond troponin and tropomyosin. *Biophys. Rev.* 10, 1121–1128 10.1007/s12551-018-0428-1 [PMCID: PMC6082317] [PubMed: 29869751] [CrossRef: 10.1007/s12551-018-0428-1]

12. Zhang Y. M., Bo J., Taffet G. E., Chang J., Shi J., Reddy A. K., Michael L. H., Schneider M. D., Entman M. L., Schwartz R. J., Wei L. (2006) Targeted deletion of ROCK1 protects the heart against pressure overload by inhibiting reactive fibrosis. *FASEB J.* 20, 916–925 10.1096/fj.05-5129com [PubMed: 16675849] [CrossRef: 10.1096/fj.05-5129com]

13. Shi J., Zhang Y. W., Summers L. J., Dorn G. W., II, Wei L. (2008) Disruption of ROCK1 gene

attenuates cardiac dilation and improves contractile function in pathological cardiac hypertrophy. *J. Mol. Cell. Cardiol.* 44, 551–560 10.1016/j.yjmcc.2007.11.018 [PMCID: PMC2728597] [PubMed: 18178218] [CrossRef: 10.1016/j.yjmcc.2007.11.018]

14. Chang J., Xie M., Shah V. R., Schneider M. D., Entman M. L., Wei L., Schwartz R. J. (2006) Activation of Rho-associated coiled-coil protein kinase 1 (ROCK-1) by caspase-3 cleavage plays an essential role in cardiac myocyte apoptosis. *Proc. Natl. Acad. Sci. USA* 103, 14495–14500 10.1073/pnas.0601911103 [PMCID: PMC1599988] [PubMed: 16983089] [CrossRef: 10.1073/pnas.0601911103]

15. Shi J., Zhang L., Wei L. (2011) Rho-kinase in development and heart failure: insights from genetic models. *Pediatr. Cardiol.* 32, 297–304 10.1007/s00246-011-9920-0 [PMCID: PMC3085170] [PubMed: 21327630] [CrossRef: 10.1007/s00246-011-9920-0]

16. Shi J., Zhang Y. W., Yang Y., Zhang L., Wei L. (2010) ROCK1 plays an essential role in the transition from cardiac hypertrophy to failure in mice. *J. Mol. Cell. Cardiol.* 49, 819–828 10.1016/j.yjmcc.2010.08.008 [PMCID: PMC2949495] [PubMed: 20709073] [CrossRef: 10.1016/j.yjmcc.2010.08.008]

17. Shi J., Surma M., Wei L. (2018) Disruption of ROCK1 gene restores autophagic flux and mitigates doxorubicin-induced cardiotoxicity. *Oncotarget* 9, 12995–13008 10.18632/oncotarget.24457 [PMCID: PMC5849190] [PubMed: 29560126] [CrossRef: 10.18632/oncotarget.24457]

18. Yang X., Li Q., Lin X., Ma Y., Yue X., Tao Z., Wang F., Mckeehan W. L., Wei L., Schwartz R. J., Chang J. (2012) Mechanism of fibrotic cardiomyopathy in mice expressing truncated Rho-associated coiled-coil protein kinase 1. *FASEB J.* 26, 2105–2116 10.1096/fj.11-201319 [PMCID: PMC3336781] [PubMed: 22278938] [CrossRef: 10.1096/fj.11-201319]

19. Rikitake Y., Oyama N., Wang C. Y., Noma K., Satoh M., Kim H. H., Liao J. K. (2005) Decreased perivascular fibrosis but not cardiac hypertrophy in ROCK1+/- haploinsufficient mice. *Circulation* 112, 2959–2965 10.1161/CIRCULATIONAHA.105.584623 [PMCID: PMC2640100] [PubMed: 16260635] [CrossRef: 10.1161/CIRCULATIONAHA.105.584623]

20. Okamoto R., Li Y., Noma K., Hiroi Y., Liu P. Y., Taniguchi M., Ito M., Liao J. K. (2013) FHL2 prevents cardiac hypertrophy in mice with cardiac-specific deletion of ROCK2. *FASEB J.* 27, 1439–1449 10.1096/fj.12-217018 [PMCID: PMC3606529] [PubMed: 23271052] [CrossRef: 10.1096/fj.12-217018]

21. Sunamura S., Satoh K., Kurosawa R., Ohtsuki T., Kikuchi N., Elias-Al-Mamun M., Shimizu T., Ikeda S., Suzuki K., Satoh T., Omura J., Nogi M., Numano K., Siddique M. A. H., Miyata S., Miura M., Shimokawa H. (2018) Different roles of myocardial ROCK1 and ROCK2 in cardiac dysfunction and

postcapillary pulmonary hypertension in mice. *Proc. Natl. Acad. Sci. USA* 115, E7129–E7138 10.1073/pnas.1721298115 [PMCID: PMC6064988] [PubMed: 29987023] [CrossRef: 10.1073/pnas.1721298115]

22. Sohal D. S., Nghiem M., Crackower M. A., Witt S. A., Kimball T. R., Tymitz K. M., Penninger J. M., Molkentin J. D. (2001) Temporally regulated and tissue-specific gene manipulations in the adult and embryonic heart using a tamoxifen-inducible Cre protein. *Circ. Res.* 89, 20–25 10.1161/hh1301.092687 [PubMed: 11440973] [CrossRef: 10.1161/hh1301.092687]

23. Shi J., Wu X., Surma M., Vemula S., Zhang L., Yang Y., Kapur R., Wei L. (2013) Distinct roles for ROCK1 and ROCK2 in the regulation of cell detachment. *Cell Death Dis.* 4, e483 10.1038/cddis.2013.10 [PMCID: PMC3734810] [PubMed: 23392171] [CrossRef: 10.1038/cddis.2013.10]

24. Agah R., Frenkel P. A., French B. A., Michael L. H., Overbeek P. A., Schneider M. D. (1997) Gene recombination in postmitotic cells. Targeted expression of Cre recombinase provokes cardiac-restricted, site-specific rearrangement in adult ventricular muscle in vivo. *J. Clin. Invest.* 100, 169–179 10.1172/JCI119509 [PMCID: PMC508177] [PubMed: 9202069] [CrossRef: 10.1172/JCI119509]

25. Shi J., Zhang L., Zhang Y. W., Surma M., Mark Payne R., Wei L. (2012) Downregulation of doxorubicin-induced myocardial apoptosis accompanies postnatal heart maturation. *Am. J. Physiol. Heart Circ. Physiol.* 302, H1603–H1613 10.1152/ajpheart.00844.2011 [PMCID: PMC3330803] [PubMed: 22328080] [CrossRef: 10.1152/ajpheart.00844.2011]

26. Hall M. E., Smith G., Hall J. E., Stec D. E. (2011) Systolic dysfunction in cardiac-specific ligand-inducible MerCreMer transgenic mice. *Am. J. Physiol. Heart Circ. Physiol.* 301, H253–H260 10.1152/ajpheart.00786.2010 [PMCID: PMC3129917] [PubMed: 21536850] [CrossRef: 10.1152/ajpheart.00786.2010]

27. Lexow J., Poggioli T., Sarathchandra P., Santini M. P., Rosenthal N. (2013) Cardiac fibrosis in mice expressing an inducible myocardial-specific Cre driver. *Dis. Model. Mech.* 6, 1470–1476 10.1242/dmm.010470 [PMCID: PMC3820269] [PubMed: 23929940] [CrossRef: 10.1242/dmm.010470]

28. Bersell K., Choudhury S., Mollova M., Polizzotti B. D., Ganapathy B., Walsh S., Wadugu B., Arab S., Kühn B. (2013) Moderate and high amounts of tamoxifen in αMHC-MerCreMer mice induce a DNA damage response, leading to heart failure and death. *Dis. Model. Mech.* 6, 1459–1469 10.1242/dmm.010447 [PMCID: PMC3820268] [PubMed: 23929941] [CrossRef: 10.1242/dmm.010447]

29. Kim Y. C., Guan K. L. (2015) mTOR: a pharmacologic target for autophagy regulation. *J. Clin.*

Invest. 125, 25–32 10.1172/JCI73939 [PMCID: PMC4382265] [PubMed: 25654547] [CrossRef: 10.1172/JCI73939]

30. Nacarelli T., Azar A., Sell C. (2015) Aberrant mTOR activation in senescence and aging: a mitochondrial stress response? *Exp. Gerontol.* 68, 66–70 10.1016/j.exger.2014.11.004 [PMCID: PMC4589173] [PubMed: 25449851] [CrossRef: 10.1016/j.exger.2014.11.004]

31. Sciarretta S., Forte M., Frati G., Sadoshima J. (2018) New insights into the role of mTOR signaling in the cardiovascular system. *Circ. Res.* 122, 489–505 10.1161/CIRCRESAHA.117.311147 [PMCID: PMC6398933] [PubMed: 29420210] [CrossRef: 10.1161/CIRCRESAHA.117.311147]

32. Pugach E. K., Richmond P. A., Azofeifa J. G., Dowell R. D., Leinwand L. A. (2015) Prolonged Cre expression driven by the α-myosin heavy chain promoter can be cardiotoxic. *J. Mol. Cell. Cardiol.* 86, 54–61 10.1016/j.yjmcc.2015.06.019 [PMCID: PMC4558343] [PubMed: 26141530] [CrossRef: 10.1016/j.yjmcc.2015.06.019]

33. Shi J., Wei L. (2007) Rho kinase in the regulation of cell death and survival. *Arch. Immunol. Ther. Exp. (Warsz.)* 55, 61–75 10.1007/s00005-007-0009-7 [PMCID: PMC2612781] [PubMed: 17347801] [CrossRef: 10.1007/s00005-007-0009-7]

34. Wei L., Surma M., Shi S., Lambert-Cheatham N., Shi J. (2016) Novel insights into the roles of Rho kinase in cancer. *Arch. Immunol. Ther. Exp. (Warsz.)* 64, 259–278 10.1007/s00005-015-0382-6 [PMCID: PMC4930737] [PubMed: 26725045] [CrossRef: 10.1007/s00005-015-0382-6]

35. Del Re D. P., Miyamoto S., Brown J. H. (2008) Focal adhesion kinase as a RhoA-activable signaling scaffold mediating Akt activation and cardiomyocyte protection. *J. Biol. Chem.* 283, 35622–35629 10.1074/jbc.M804036200 [PMCID: PMC2602897] [PubMed: 18854312] [CrossRef: 10.1074/jbc.M804036200]

36. Torsoni A. S., Marin T. M., Velloso L. A., Franchini K. G. (2005) RhoA/ROCK signaling is critical to FAK activation by cyclic stretch in cardiac myocytes. *Am. J. Physiol. Heart Circ. Physiol.* 289, H1488–H1496 10.1152/ajpheart.00692.2004 [PubMed: 15923313] [CrossRef: 10.1152/ajpheart.00692.2004]

37. Shirakabe A., Ikeda Y., Sciarretta S., Zablocki D. K., Sadoshima J. (2016) Aging and autophagy in the heart. *Circ. Res.* 118, 1563–1576 10.1161/CIRCRESAHA.116.307474 [PMCID: PMC4869999] [PubMed: 27174950] [CrossRef: 10.1161/CIRCRESAHA.116.307474]

38. Eisenberg T., Abdellatif M., Schroeder S., Primessnig U., Stekovic S., Pendl T., Harger A., Schipke J., Zimmermann A., Schmidt A., Tong M., Ruckenstuhl C., Dammbrueck C., Gross A. S., Herbst V., Magnes C., Trausinger G., Narath S., Meinitzer A., Hu Z., Kirsch A., Eller K., Carmona-Gutierrez D., Büttner S., Pietrocola F., Knittelfelder O., Schrepfer E., Rockenfeller P., Simonini C., Rahn A., Horsch M., Moreth

K., Beckers J., Fuchs H., Gailus-Durner V., Neff F., Janik D., Rathkolb B., Rozman J., de Angelis M. H., Moustafa T., Haemmerle G., Mayr M., Willeit P., von Frieling-Salewsky M., Pieske B., Scorrano L., Pieber T., Pechlaner R., Willeit J., Sigrist S. J., Linke W. A., Mühlfeld C., Sadoshima J., Dengjel J., Kiechl S., Kroemer G., Sedej S., Madeo F. (2016) Cardioprotection and lifespan extension by the natural polyamine spermidine. *Nat. Med.* 22, 1428–1438 10.1038/nm.4222 [PMCID: PMC5806691] [PubMed: 27841876] [CrossRef: 10.1038/nm.4222]

39. Sciarretta S., Volpe M., Sadoshima J. (2014) Mammalian target of rapamycin signaling in cardiac physiology and disease. *Circ. Res.* 114, 549–564 10.1161/CIRCRESAHA.114.302022 [PMCID: PMC3995130] [PubMed: 24481845] [CrossRef: 10.1161/CIRCRESAHA.114.302022]

40. Lauriol J., Keith K., Jaffré F., Couvillon A., Saci A., Goonasekera S. A., McCarthy J. R., Kessinger C. W., Wang J., Ke Q., Kang P. M., Molkentin J. D., Carpenter C., Kontaridis M. I. (2014) RhoA signaling in cardiomyocytes protects against stress-induced heart failure but facilitates cardiac fibrosis. *Sci. Signal.* 7, ra100 10.1126/scisignal.2005262 [PMCID: PMC4300109] [PubMed: 25336613] [CrossRef: 10.1126/scisignal.2005262]

41. Takefuji M., Krüger M., Sivaraj K. K., Kaibuchi K., Offermanns S., Wettschureck N. (2013) RhoGEF12 controls cardiac remodeling by integrating G protein- and integrin-dependent signaling cascades. *J. Exp. Med.* 210, 665–673 10.1084/jem.20122126 [PMCID: PMC3620351] [PubMed: 23530122] [CrossRef: 10.1084/jem.20122126]

42. Gurkar A. U., Chu K., Raj L., Bouley R., Lee S. H., Kim Y. B., Dunn S. E., Mandinova A., Lee S. W. (2013) Identification of ROCK1 kinase as a critical regulator of Beclin1-mediated autophagy during metabolic stress. *Nat. Commun.* 4, 2189 10.1038/ncomms3189 [PMCID: PMC3740589] [PubMed: 23877263] [CrossRef: 10.1038/ncomms3189]

43. Mleczak A., Millar S., Tooze S. A., Olson M. F., Chan E. Y. (2013) Regulation of autophagosome formation by Rho kinase. *Cell. Signal.* 25, 1–11 10.1016/j.cellsig.2012.09.010 [PubMed: 22975682] [CrossRef: 10.1016/j.cellsig.2012.09.010]

44. Bauer P. O., Wong H. K., Oyama F., Goswami A., Okuno M., Kino Y., Miyazaki H., Nukina N. (2009) Inhibition of Rho kinases enhances the degradation of mutant huntingtin. *J. Biol. Chem.* 284, 13153–13164 10.1074/jbc.M809229200 [PMCID: PMC2676047] [PubMed: 19278999] [CrossRef: 10.1074/jbc.M809229200]

45. Aguilera M. O., Berón W., Colombo M. I. (2012) The actin cytoskeleton participates in the early events of autophagosome formation upon starvation induced autophagy. *Autophagy* 8, 1590–1603 10.4161/auto.21459 [PMCID: PMC3494589] [PubMed: 22863730] [CrossRef: 10.4161/auto.21459]

Figures and Tables

Figure 1

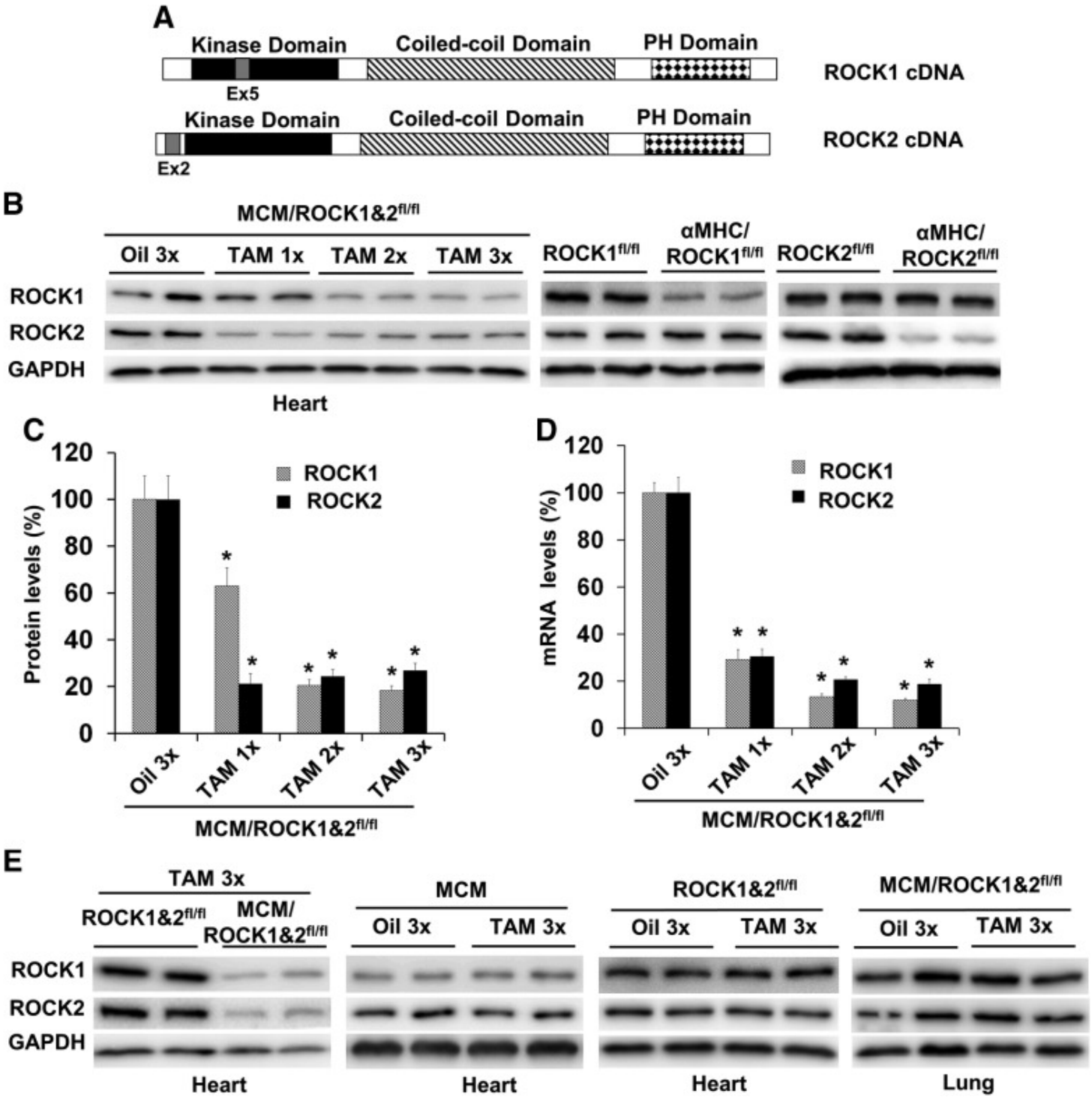

Inducible cardiomyocyte-specific deletion of both ROCK1 and ROCK2 by TAM treatment. *A*) Schematic representation of the domain structures of ROCK1 and ROCK2 indicating the positions of exon 5 for ROCK1 and exon 2 for ROCK2, which can be deleted by Cre recombinase, resulting in ROCK1 and ROCK2 deletion. *B*) Representative image of Western blot of ROCK1 and ROCK2 in the ventricular homogenates from fl/fl fl/fl fl/fl fl/fl fl/fl

MCM/ROCK1 ROCK2 (MCM/ROCK1&2), α-MHC–Cre/ROCK1 , or α-MHC–Cre/ROCK2 mice at 3 mo of age. MCM/ROCK1&2$^{fl/fl}$ mice were subjected to 1–3 injections (1/d) of TAM or oil and collected 5 d from the first injection. *C*) Quantitative analysis of the Western blots showing that the maximal reduction of ROCK1 and ROCK2 protein levels can be reached in the MCM/ROCK1&2$^{fl/fl}$ heart lysates after 2 injections. The expression of ROCK1 and ROCK2 was normalized to that of GAPDH. *D*) qRT-PCR analysis of ROCK1 and ROCK2 in the same heart samples used for the Western blot analysis. The expression of ROCK1 and ROCK2 was normalized to that of GAPDH. *E*) Representative image of Western blot of ROCK1 and ROCK2 in the ventricular or lung homogenates from MCM/ROCK1&2$^{fl/fl}$, ROCK1$^{fl/fl}$ROCK2$^{fl/fl}$ (ROCK1&2$^{fl/fl}$), or MCM mice subjected to 3 injections of TAM or oil and collected 5 d from the first injection; n = 4–6 in each group. *P < 0.05 *vs.* oil-injected group.

Figure 2

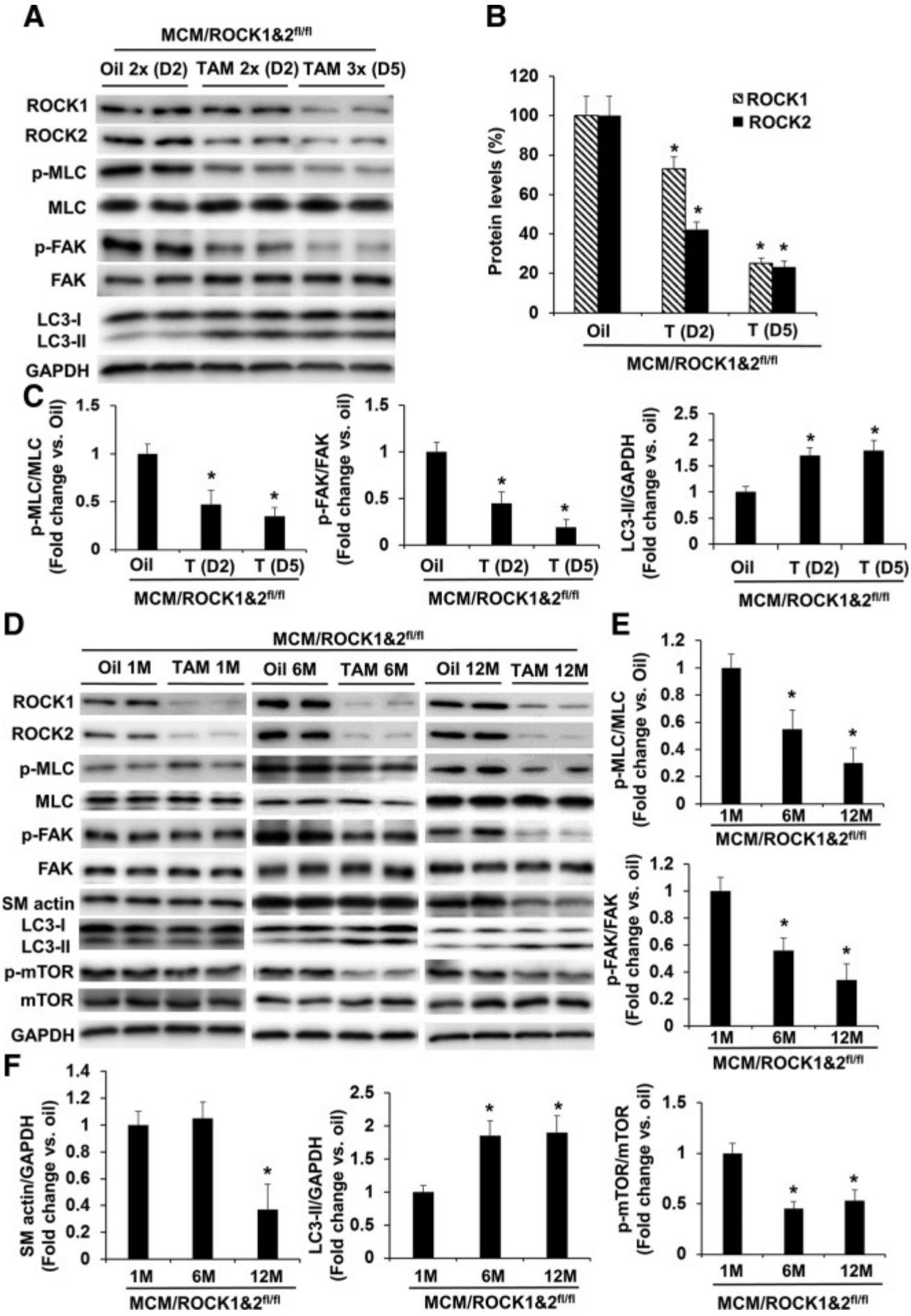
A
MCM/ROCK1&2fl/fl
Oil 2x (D2)
TAM 2x (D2)
TAM 3x (D5)
ROCK1
ROCK2
p-MLC
MLC
p-FAK
FAK
LC3-I
LC3-II
GAPDH
B
ROCK1
ROCK2
Protein levels (%)
Oil
T (D2)
T (D5)
MCM/ROCK1&2fl/fl
C
p-MLC/MLC (Fold change vs. Oil)
p-FAK/FAK (Fold change vs. oil)
LC3-II/GAPDH (Fold change vs. oil)
Oil
T (D2)
T (D5)
MCM/ROCK1&2fl/fl
D
MCM/ROCK1&2fl/fl
Oil 1M
TAM 1M
Oil 6M
TAM 6M
Oil 12M
TAM 12M
ROCK1
ROCK2
p-MLC
MLC
p-FAK
FAK
SM actin
LC3-I
LC3-II
p-mTOR
mTOR
GAPDH
E
p-MLC/MLC (Fold change vs. Oil)
p-FAK/FAK (Fold change vs. oil)
1M
6M
12M
MCM/ROCK1&2fl/fl
F
SM actin/GAPDH (Fold change vs. oil)
LC3-II/GAPDH (Fold change vs. oil)
p-mTOR/mTOR (Fold change vs. oil)
1M
6M
12M
MCM/ROCK1&2fl/fl

Molecular changes following inducible cardiomyocyte-specific deletion of both ROCK1 and ROCK2. *A*) Representative image of Western blot analysis in the ventricular homogenates from MCM/ROCK1$^{fl/fl}$ROCK2$^{fl/fl}$ (MCM/ROCK1&2$^{fl/fl}$) mice subjected to 2 or 3 injections (1/d) of TAM and collected 2 or 5 d from the first injection, respectively, showing progressive reduction of ROCK1, ROCK2, phosphorylation of MLC and FAK, and increases in autophagy marker LC3-II. *B*) Quantitative analysis of immunoreactive bands of ROCK1 and ROCK2. *C*) Quantitative analysis of immunoreactive bands of p-MLC and MLC, p-FAK and FAK, and LC3-II. *D*) Representative image of Western blot analysis in the ventricular homogenates from MCM/ROCK1&2$^{fl/fl}$ mice collected 1, 6, or 12 mo from the TAM or oil injection. *E*) Quantitative analysis of immunoreactive bands of p-MLC and MLC and p-FAK and FAK. *F*) Quantitative analysis of immunoreactive bands of SM actin, LC3-II, and p-mTOR and mTOR; n = 4–6 in each group. *P < 0.05 *vs.* oil-injected group of same age.

Figure 3

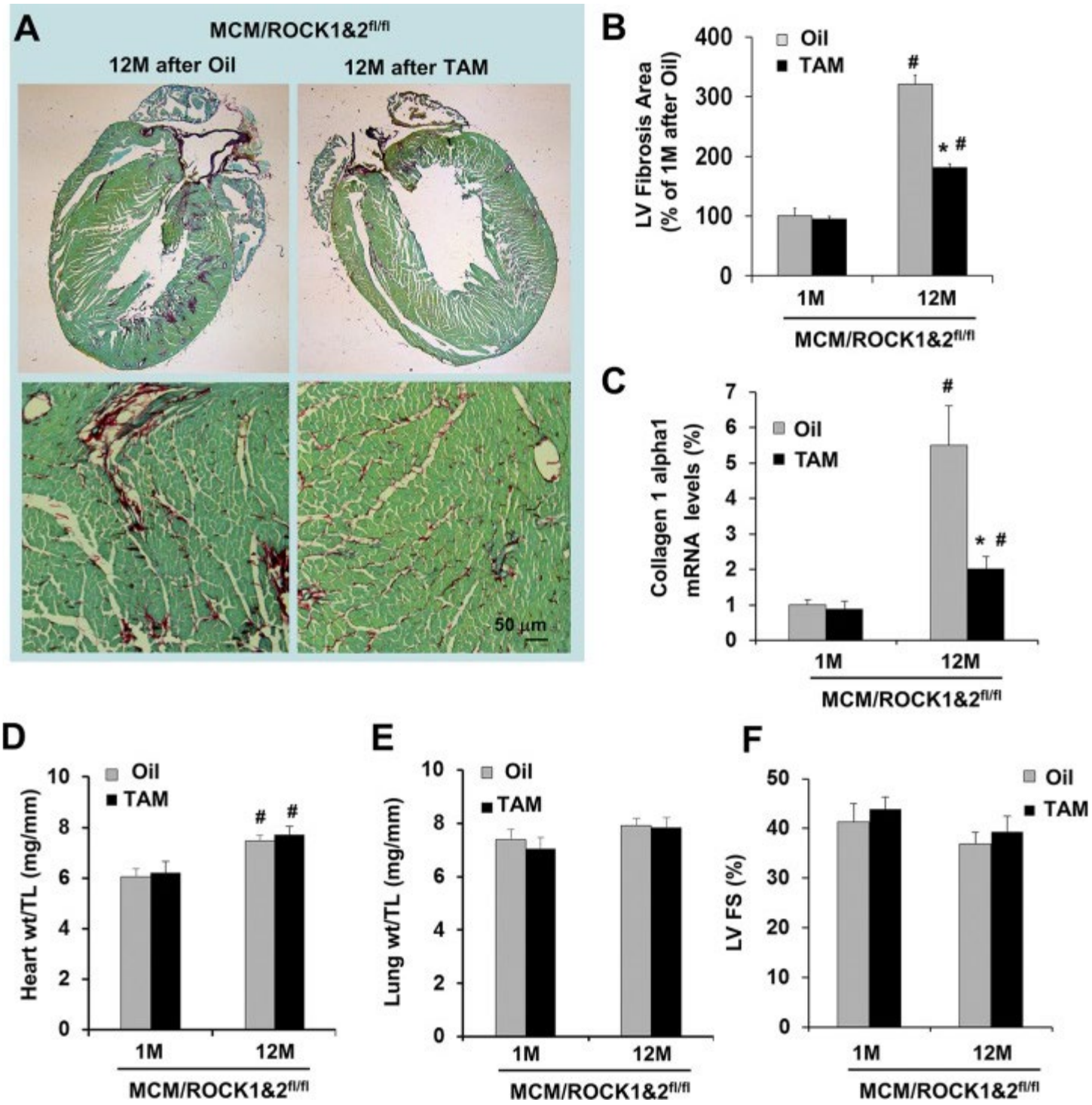

Cardiomyocyte-specific deletion of both ROCK1 and ROCK2 reduces age-related cardiac fibrosis. *A*) Representative heart sections stained with picrosirius red/fast green (scale bar, 50 μm) showing collagen deposition in 18-mo-old MCM/ROCK1$^{fl/fl}$ROCK2$^{fl/fl}$ (MCM/ROCK1&2$^{fl/fl}$) hearts collected 12 mo after TAM or oil injection received at 6 mo of age. *B*) Quantitative analysis of the collagen deposition in 7- or 18-mo-old MCM/ROCK1&2$^{fl/fl}$ hearts collected 1 or 12 mo after TAM or oil injection received at 6 mo of age, expressed as a percentage change relative to oil-injected hearts collected 1 mo after injection (4–6 hearts in each group). *C*) qRT-PCR analysis of collagen type 1α1 normalized to that of GAPDH. The mean normalized value in oil-injected hearts was defined as 1.0. *D*) Quantitative analysis of heart weight (heart

wt) to tibial length (TL) ratios. *E*) Quantitative analysis of lung weight (lung wt) to TL ratios. *F*) M-mode echocardiography was performed in series at 1 or 12 mo from TAM or oil injection received at 6 mo of age. LV FS, left ventricular fractional shortening; n = 6–8 in each group. *$P < 0.05$ *vs.* oil-injected group of same age, $^{\#}P < 0.05$ *vs.* 1-mo group of same treatment.

Figure 4

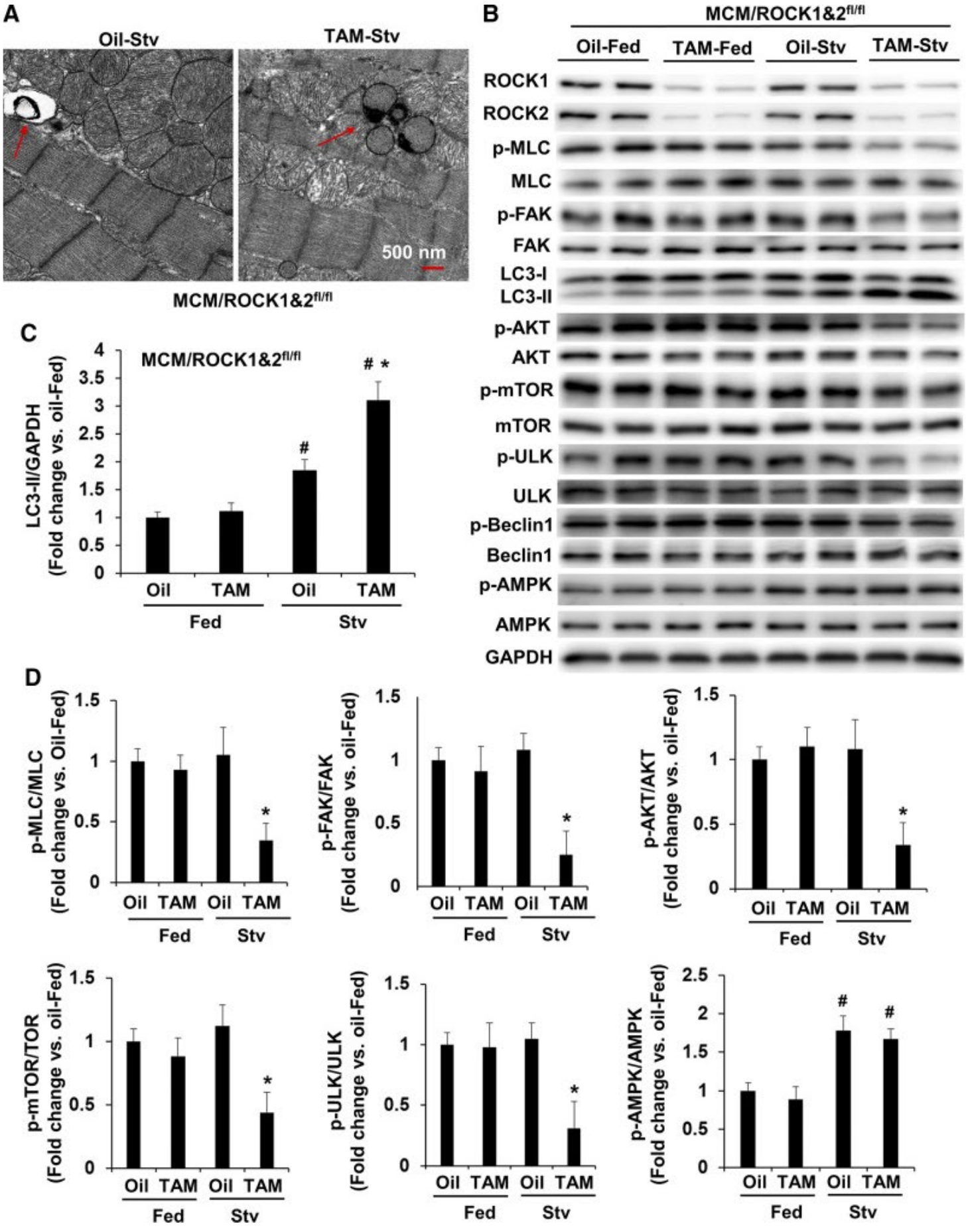

Cardiomyocyte-specific deletion of both ROCK1 and ROCK2 promotes starvation-induced autophagy

through inhibiting mTOR signaling. *A*) Starvation was performed for 24 h on MCM/ROCK1$^{fl/fl}$ROCK2$^{fl/fl}$ (MCM/ROCK1&2$^{fl/fl}$) mice after 30 d from first TAM or oil injection. Representative transmission electron microscopy images of MCM/ROCK1&2$^{fl/fl}$ hearts collected after 24 h of starvation. TAM-injected starved MCM/ROCK1&2$^{fl/fl}$ hearts showed increased numbers of autophagic vacuoles (red arrows) compared with oil-injected starved MCM/ROCK1&2$^{fl/fl}$ hearts. Scale bar, 500 nm. *B*) Representative image of Western blot analysis in the ventricular homogenates from fed or starved mice. *C*) Quantitative analysis of immunoreactive bands of LC3-II. *D*) Quantitative analysis of p-MLC and MLC, p-FAK and FAK, p-AKT and AKT, p-mTOR and mTOR, p-ULK and ULK, and p-AMPK and AMPK. Stv, starved; $n = 4–6$ in each group. *$P < 0.05$ *vs.* oil-injected group, $^{\#}P < 0.05$ *vs.* fed group.

Figure 5

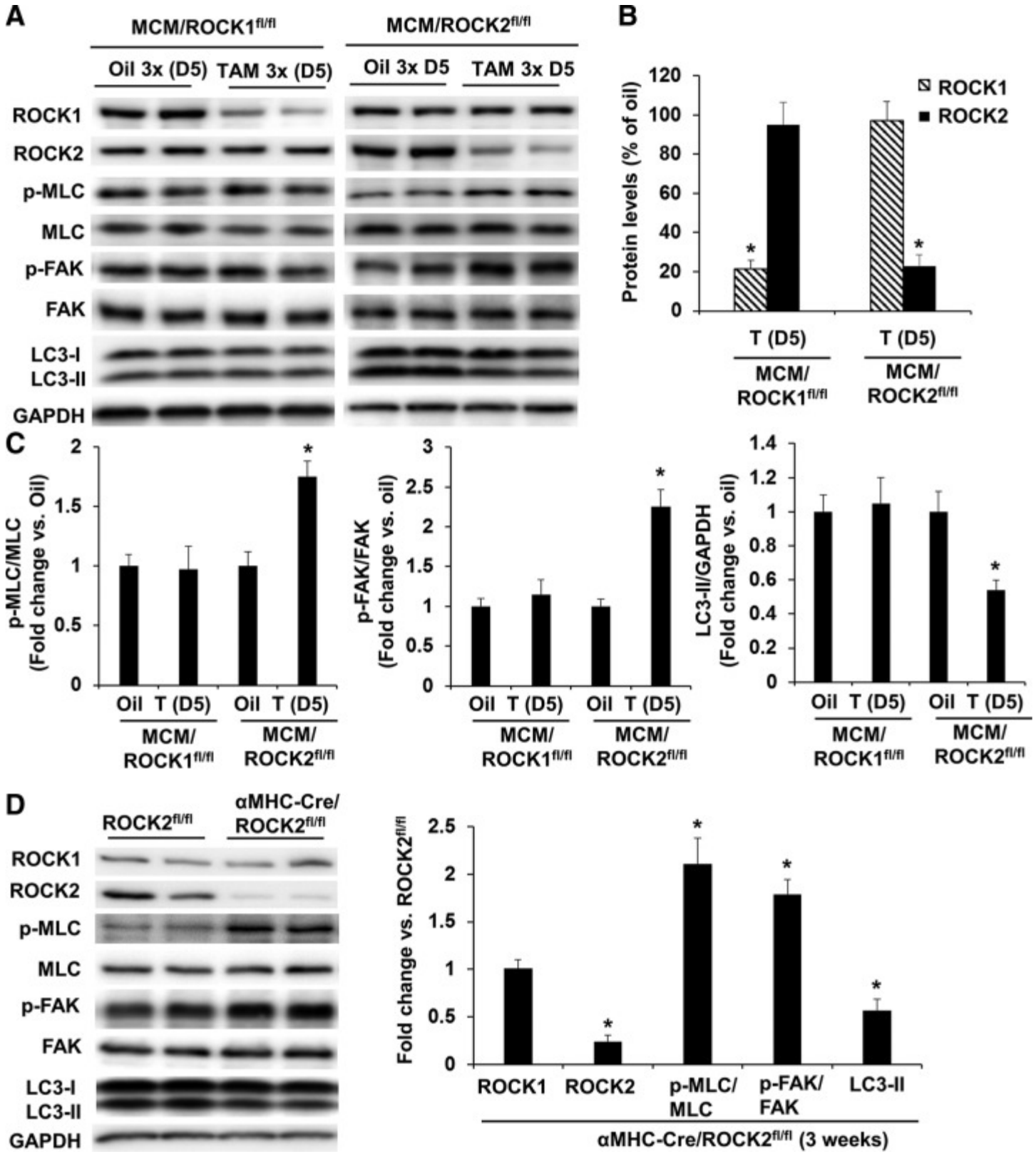

Inducible cardiomyocyte-specific deletion of ROCK2 induces a compensatory increase in ROCK1 activity. *A*) Representative image of Western blot of ROCK1, ROCK2, p-MLC, MLC, p-FAK, FAK, and LC3 in the ventricular homogenates from MCM/ROCK1$^{fl/fl}$ or MCM/ROCK2$^{fl/fl}$ mice subjected to 3 injections of TAM and collected 5 d from the first injection, showing reduction of ROCK1 or ROCK2 in MCM/ROCK1$^{fl/fl}$ or MCM/ROCK2$^{fl/fl}$ hearts, respectively, increases in phosphorylation of MLC and FAK, and reduction of

LC3B-II in MCM/ROCK2 hearts. *B*) Quantitative analysis of immunoreactive bands of ROCK1 and ROCK2. *C*) Quantitative analysis of immunoreactive bands of p-MLC and MLC, p-FAK and FAK, and LC3-II; n = 4–6 in each group. *$P < 0.05$ *vs.* oil-injected group with same genotype. *D*) Representative image (left) and quantitative analysis (right) of Western blot of ROCK1, ROCK2, p-MLC, MLC, p-FAK, FAK, and LC3B in the ventricular homogenates from α-MHC–Cre/ROCK2$^{fl/fl}$ mice at 3 wk of age; n = 4–6 in each group. *$P <$ 0.05 *vs.* ROCK2$^{fl/fl}$ group.

Figure 6

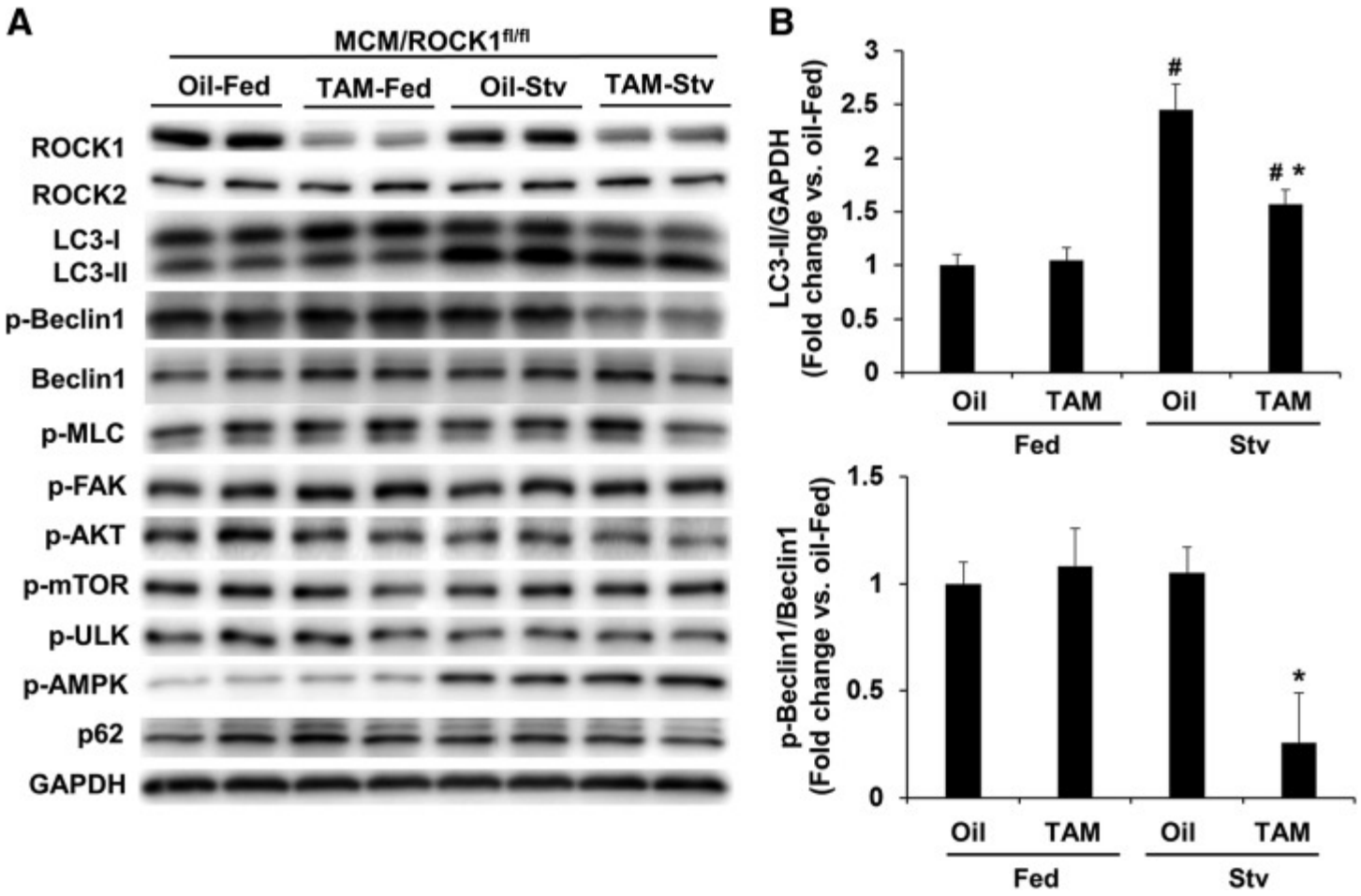

Inducible cardiomyocyte-specific deletion of ROCK1 inhibits starvation-induced autophagy through inhibiting Beclin 1 activation. *A*) Starvation was performed for 24 h on MCM/ROCK1$^{fl/fl}$ mice 30 d after the first TAM or oil injection. Representative image of Western blot of ROCK1, ROCK2, p-MLC, p-FAK, LC3, p-AKT, p-mTOR, p-ULK, p–Beclin 1, Beclin 1, p-AMPK, and p62 in the ventricular homogenates from fed or starved mice. *B*) Quantitative analysis of immunoreactive bands of LC3-II, p–Beclin 1, and Beclin 1. Stv, starved; n = 4–6 in each group. *$P < 0.05$ *vs.* oil-injected group, $^{\#}P < 0.05$ *vs.* fed group.

Figure 7

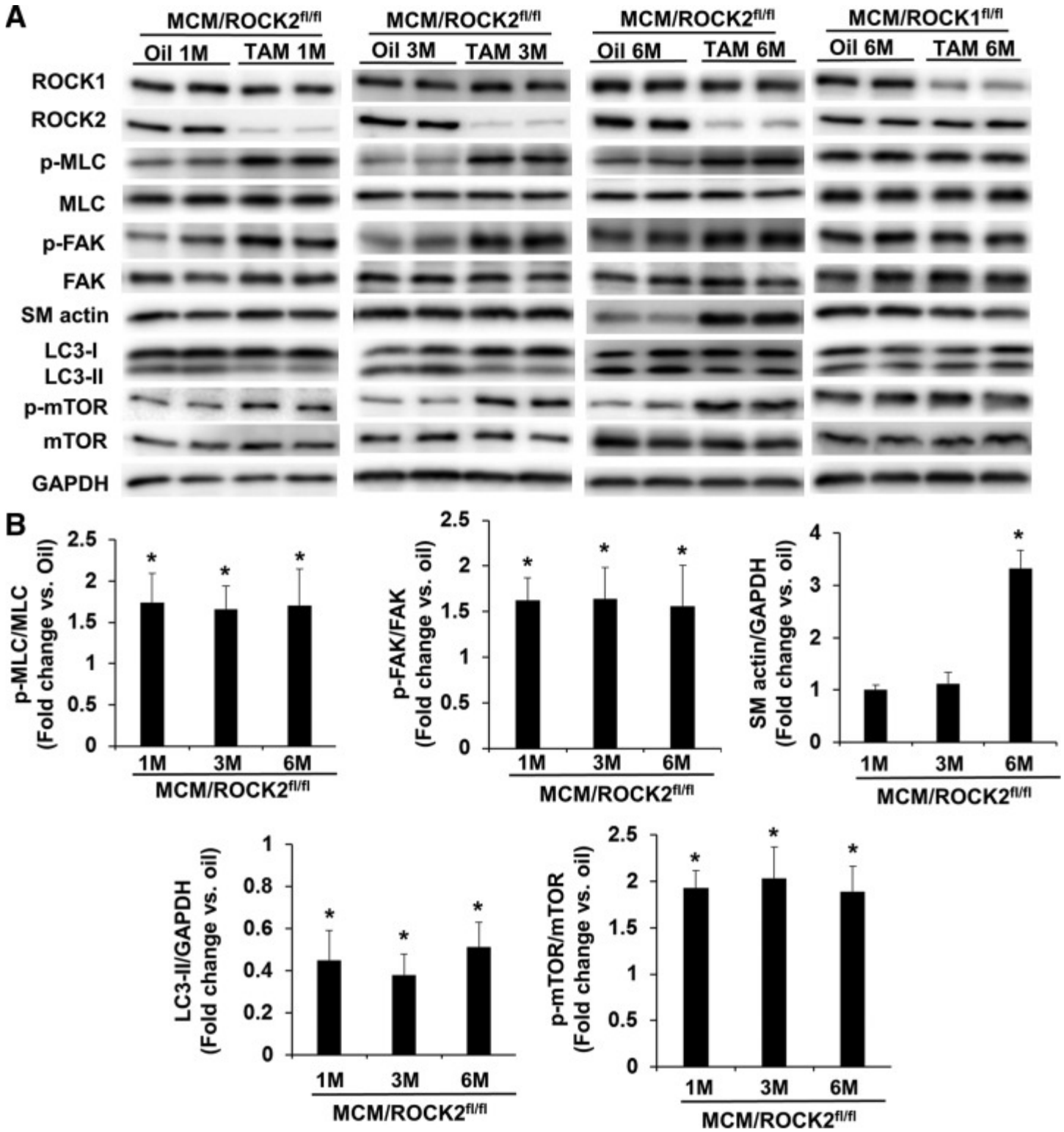

Late molecular changes following inducible cardiomyocyte-specific deletion of ROCK2. *A*) Representative image of Western blot of ROCK1, ROCK2, p-MLC, MLC, p-FAK, FAK, smooth-muscle α-actin (SM actin), LC3, p-mTOR, and mTOR in the ventricular homogenates from 7-, 9-, or 12-mo-old MCM/ROCK2$^{fl/fl}$ mice collected 1, 3, or 6 mo after the TAM or oil injection received at 6 mo of age or from 12-mo-old MCM/ROCK1$^{fl/fl}$ mice collected 6 mo after the TAM or oil injection. *B*) Quantitative analysis of immunoreactive bands of p-MLC and MLC, p-FAK and FAK, SM actin, LC3-II, and p-mTOR and mTOR; n = 4–6 in each group. *$P < 0.05$ *vs.* oil-injected group of same genotype.

Figure 8

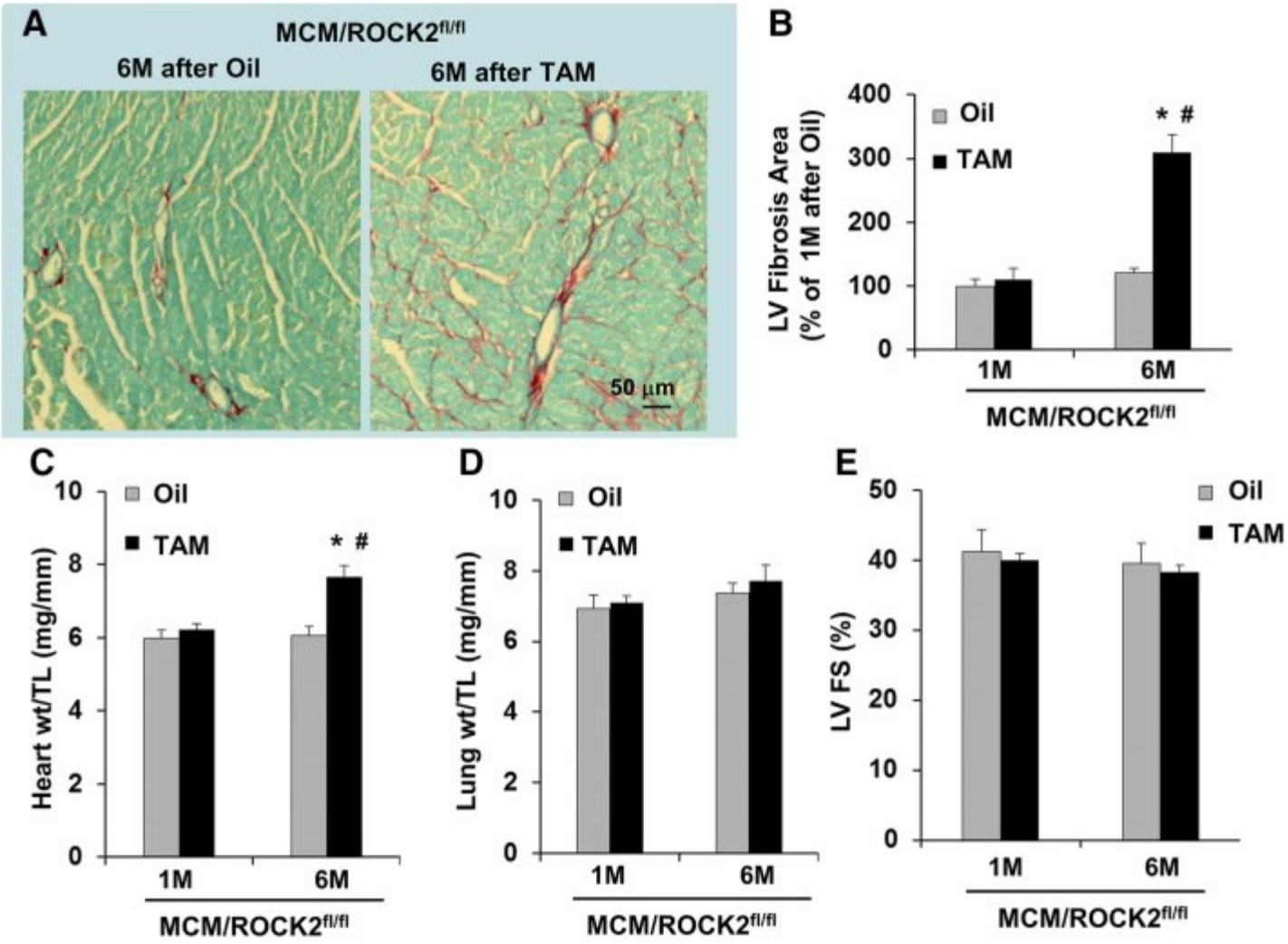

Cardiomyocyte-specific deletion of ROCK2 induces age-related cardiac fibrosis. *A*) Representative heart sections stained with picrosirius red and fast green showing collagen deposition in 12-mo-old MCM and ROCK2$^{fl/fl}$ hearts collected 6 mo after TAM or oil injection that MCM/ROCK2$^{fl/fl}$ mice received at 6 mo of age (scale bar, 50 μm). *B*) Quantitative analysis of the collagen deposition in 7- or 12-mo-old MCM/ROCK2$^{fl/fl}$ hearts collected 1 or 6 mo after TAM or oil injection received at 6 mo of age. *C*) Quantitative analysis of heart weight (heart wt) to tibial length (TL) ratios. *D*) Quantitative analysis of lung weight (lung wt) to TL ratios. *E*) M-mode echocardiography was performed in series at 1 or 6 mo from TAM or oil injection received at 6 mo of age. LV FS, left ventricular fractional shortening; n = 6–8 in each group. *$P < 0.05$ *vs.* oil-injected group of same age, $^{\#}P < 0.05$ *vs.* 1-mo group of same treatment.

Figure 9

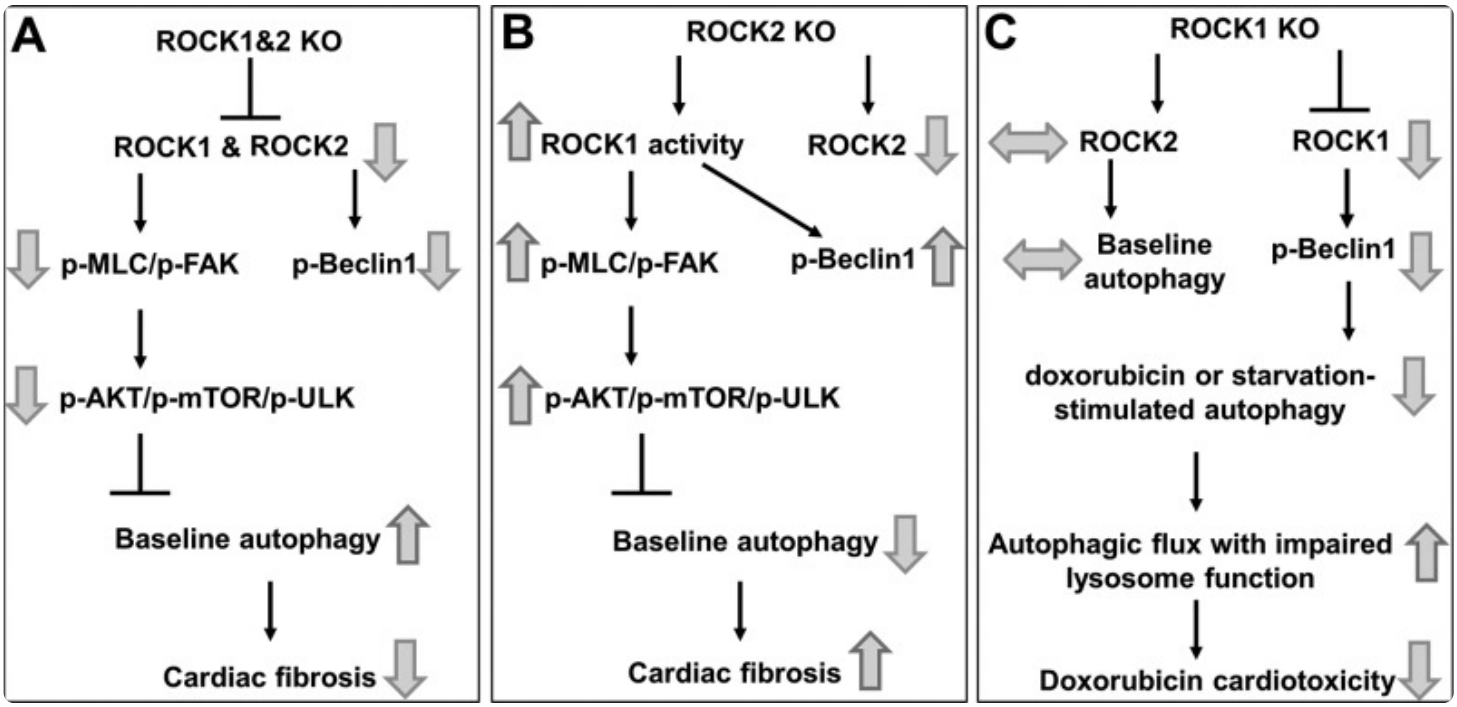

Schematic summary of roles of ROCK1 and ROCK2 in regulating nonsarcomeric cytoskeleton, autophagy, and fibrosis in cardiomyocytes. *A*) Double ROCK deletion in adult cardiomyocytes results in reduced nonsarcomeric cytoskeleton assembly (reduced p-MLC and p-FAK), resulting in increased baseline autophagy through inhibition of AKT/mTOR/ULK signaling and beneficial antifibrotic effects during the aging process. *B*) ROCK2 deletion in cardiomyocytes is profibrotic and associated with compensatory increased ROCK1 activity, which increases nonsarcomeric cytoskeleton assembly and AKT/mTOR/ULK signaling, resulting in inhibiting baseline autophagy. *C*) ROCK1 deletion in cardiomyocytes is protective in the context of doxorubicin cardiotoxicity, in part, because of reduced Beclin 1–mediated autophagy activity, resulting in improved autophagic flux when lysosome function is impaired by doxorubicin. The baseline autophagy regulated by AKT/mTOR/ULK is not affected because of the presence of ROCK2, which maintains nonsarcomeric cytoskeleton.